National Technical University Of Athens

School Of Mechanical Engineering

Control Systems Lab

Algorithms for robust grasp planning

Author:
George I. Boutselis

Supervisor:
Kostas J. Kyriakopoulos

A thesis submitted in partial fulfilment of the requirements for the degree of Diploma

in Mechanical Engineering

Athens, May 2014

[This page intentionally left blank]

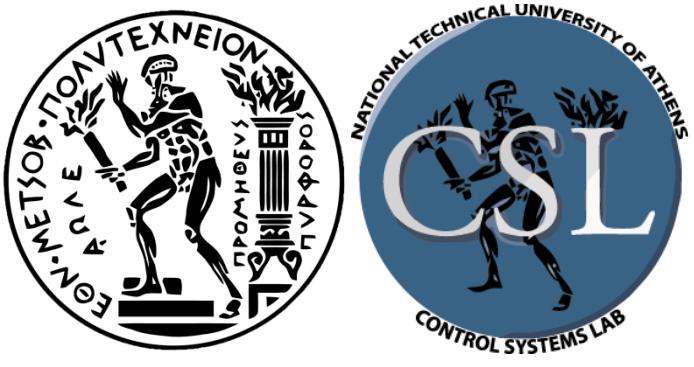

Εθνικό Μετσόβιο Πολυτεχνείο

Σχολή Μηχανολόγων Μηχανικών

Εργαστήριο Αυτομάτου Ελέγχου

Σχεδιασμός αλγορίθμων λαβής αντικειμένων για την αντιμετώπιση ενός ευρέος φάσματος αβεβαιοτήτων

Γιώργος Μπουτσέλης

Κατατέθηκε για την εκπλήρωση των υποχρεώσεων για την απόκτηση του τίτλου του Διπλωματούχου Μηχανολόγου Μηχανικού

Υπεύθυνος Καθηγητής: Κωνσταντίνος Κυριακόπουλος

Αθήνα, Μάιος 2014

Acknowledgements

Firstly, I would like to thank my advisor Professor Kostas Kyriakopoulos. I am glad that I had the opportunity to collaborate with a high caliber professor/engineer. His knowledge and experience on the field of Robotics and Controls played a key role to my work. I would, also, like to thank him for convincing me to pursue my interests through PhD studies and for giving me useful information during the application procedure.

Furthermore, I want to express my gratitude to my labmate Charalampos Bechlioulis for his great help during my work for my Diploma thesis. His willingness and patience are remarkable, especially in the beginning of our collaboration when we had to face many difficulties. Besides, his expertise on various scientific topics allowed me to gain valuable experiences. I would, also, like to thank my labmate and great researcher Minas Liarokapis. He introduced me to scientific research and was very helpful during my research assistanship at the Constrol Systems Lab. Minas encouraged me to apply for PhD studies, giving me, also, a major boost during the application phase. I feel lucky that I had the opportunity to collaborate with both of them and I am glad that our work was successful.

To proceed, I want to thank Christoforos Mavrogiannis and George Karavas. Christoforos helped me in the beginning of my diploma thesis, while both of them, and especially George, helped me complete my applications. I want to thank Agis Zisimatos and the rest of my labmates, as well, for creating a nice atmosphere.

In addition, I would like to thank my parents, John and Evridiki, my brother, Aris, my grandmothers, Nelly and Marigoula, and my girlfriend, Penny for their support during my studies.

Last but not least, I want to thank God for standing by my side through my good times and my bad times.

National Technical University Of Athens

School Of Mechanical Engineering

Diploma

Abstract

Algorithms for robust grasp planning

by George I. Boutselis

The development of human-like robotic hands has received great attention in the past. This effort aims at allowing robots to interact effectively with everyday objects, as well as perform efficiently in industrial applications. Thus, designing appropriate grasp planning algorithms is of utmost importance.

The majority of the analytical works on grasping consider both object as well as robot hand parameters to be accurately known and do not take into account the constraints imposed by the robotic hand. Obviously, the aforementioned drawbacks may lead to unsuccessful results in real applications and must be tackled properly. In this thesis, the basics of grasp analysis are presented and a complete methodology is proposed that handles the grasping problem under a wide range of uncertainties. Specifically, an acceptable posture is derived that provides robustness against positioning inaccuracies and maximizes the ability of the robot hand to exert forces on the object. In addition, in order to secure the grasp stability and lift the object properly, sufficient contact forces are determined.

Apart from focusing on deriving a stable grasp, task specificity is also addressed. More specifically, given a description of the task to be executed, the concept of Q distance is introduced in a novel way to determine an efficient grasp with a task compatible hand posture (i.e., configuration and contact points).

The efficiency of this approach is validated through simulated examples and extensive experimental paradigms using a 15 DoF DLR/HIT II robotic hand attached at the end effector of a 7 DoF Mitsubishi PA10 robotic manipulator. During the experimental phase, an appropriate tactile sensor setup, mounted on the robot hand, is utilized in order to reduce the magnitude of uncertainty regarding the grasping parameters.

Εθνικό Μετσόβιο Πολυτεχνείο

Σχολή Μηχανολόγων Μηχανικών

Γιώργος Μπουτσέλης

Διπλωματική εργασία

Σχεδιασμός αλγορίθμων λαβής αντικειμένων για την αντιμετώπιση ενός ευρέος φάσματος αβεβαιοτήτων

Περίληψη

Η ανάπτυξη ανθρωπόμορφων ρομποτικών χεριών αποτελεί ένα επιστημονικό πεδίο για το οποίο έχει παρατηρηθεί έντονο ενδιαφέρον τα τελευταία χρόνια. Αυτή η προσπάθεια στοχεύει στο να δώσει την ικανότητα στα ρομπότ να αλληλεπιδρούν με καθημερινά αντικείμενα και να έχουν υψηλές επιδόσεις σε βιομηχανικές εφαρμογές. Έτσι, ιδιαίτερη προσοχή πρέπει να δωθεί στην ανάπτυξη κατάλληλων αλγορίθμων λαβής.

Η πλειοψηφία των αναλυτικών εργασιών λαβής αντικειμένων βασίζεται στην ακριβή γνώση των παραμέτρων τόσο του αντικειμένου όσο και του ρομποτικού χεριού. Επιπλέον, οι περιορισμοί που εισάγονται από την ύπαρξη του ρομποτικού χεριού σπάνια λαμβάνονται υπόψην. Όπως γίνεται κατανοητό, τα παραπάνω ελαττώματα είναι πιθανόν να οδηγήσουν σε ανεπιτυχή αποτελέσματα και πρέπει να αντιμετωπισθούν επιτυχώς. Σε αυτή τη διπλωματική εργασία, αφού δωθούν οι βασικές έννοιες της θεωρίας λαβής αντικειμένων, αναπτύσσεται μια μεθοδολογία συνολικής αντιμετώπισης του προβλήματος της λαβής αντικειμένων υπό την ύπαρξη αβεβαιοτήτων σε παραμέτρους σχεδιασμού. Συγκεκριμένα, το αποτέλεσμα αυτής της μεθοδολογίας είναι μία αποδεκτή διαμόρφωση αρπαγής που εγγυάται την ευστάθεια της λαβής έστω και αν σφάλματα τοποθέτησης εμφανισθούν. Ακόμη, η συγκεκριμένη διαμόρφωση μεγιστοποιεί την ικανότητα του ρομποτικού χεριού να μετατρέπει ροπές σε δυνάμεις επαφής. Επιπλέον, για να ολοκληρωθεί η διαδικασία αρπαγής προτείνεται μια μεθοδολογία εύρεσης ικανοποιητικών δυνάμεων.

Εκτός από την ενασχόληση με την επίτευξη της ευστάθειας της λαβής, εξετάζεται και η περίπτωση που το ρομποτικό χέρι πρέπει να εκτελέσει μια συγκεκριμένη εργασία. Λαμβάνοντας υπόψην την περιγραφή της εργασίας, χρησιμοποιείται η

έννοια της «Q distance» για τον καθορισμό μιας διαμόρφωσης, συμβατής με τη ζητούμενη εργασία.

Η ορθότητα αυτής της προσέγγισης πιστοποιείται μέσω παραδειγμάτων προσομοίωσης και πειραματικών αποτελεσμάτων, χρησιμοποιώντας το DLR/HIT II (δεκαπέντε βαθμών ελευθερίας), το οποίο βρίσκεται στο τελικό σημείο δράσης του Mitsubishi PA10 (εφτά βαθμών ελευθερίας). Κατά τη διάρκεια της πειραματικής διαδικασίας, ένας αισθητήρας αφής χρησιμοποιείται με στόχο την μείωση του εύρους των αβεβαιοτήτων.

Contents

List of Figures

List of Tables

To my family

Chapter 1

Introduction

Nowadays, robot hands are getting more and more complex and sophisticated. Simple grippers have been largely replaced by state-of-the-art, multifingered, human- like robot hands with many degrees of freedom and high levels of dexterity. Consequently, there arises the need for the design of corresponding, equivalently complex and general algorithms that can efficiently control robot hands and exploit the capabilities of their hardware.

In this direction, specific emphasis has been devoted to the fundamental problem of robot grasping. Grasping, an essential requirement for almost every manipulation task is a complex problem of mechanics which can be approached by many different points of view. Besides, human experience has proven that an object can be grasped in many different ways depending on the task that we need to execute. However, as humans grow older and get more and more aware of their environment as well as of their body, they adopt intuitive optimization schemes, so that they grasp objects consuming the least possible amount of energy and facilitating the desired task execution.

Inspired by this simple idea, this thesis addresses the problem of the grasp optimization, taking into consideration the geometrical and mechanical constraints imposed by the hand's design and the grasped object's surface properties. In addition, uncertainties that may occur during the grasp implementation are considered.

1.1 Robotic hands

The evolution of the design of robotic hands has led to the creation of state-of-the-art multifingered robot hands which can play a significant role in many areas. The trend of imitating the complex nature of the human hand has led many companies to build

different types of hands, incorporating different types of technologies. One of the frst and most widely known multifingered robot hands was the three-fingered Barrett Hand, developed by Barrett Technology Inc illustrated in Fig. 1.1. Some of today's most representative robot hands have been developed by NASA [1], DLR [2] and DLR/HIT [3], [4]. In general, the modern human-like robot hands can be separated in two main categories depending on their type of actuation:

- External actuation robotic hands in which all the actuators are mounted in the forearm
- Internal actuation robotic hands in which all the actuators are integrated in the finger body and the palm

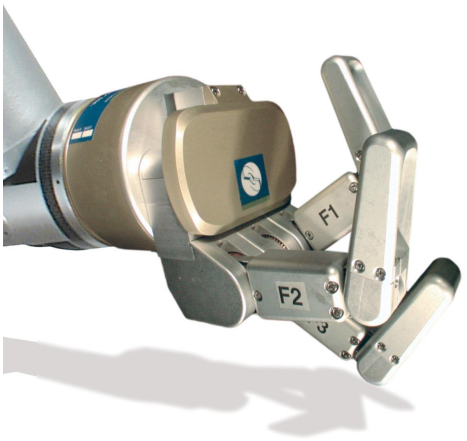

FIGURE 1.1: Barrett Robotic Hand, Barrett Technology Inc

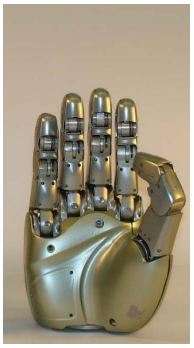

FIGURE 1.2: DLR HIT II

FIGURE 1.3: Robonaut

Due to their fundamental differences in actuation, in the first category the hand body is usually bigger than in the latter. Hence, in order for the Internal Actuation Robotic Hands to be more competitive, it is important that they are built in smaller dimensions. The reduction of the motor's and circuits' size is crucial in this direction.

1.2 Grasp planning

During the 80's and early 90's, roboticists were devoted to the study of the Grasp Analysis, paying more attention to the complex mechanics of the problem and the formulation of grasp optimization problems. Since grasping constituted a new research direction, this was necessary and very important. However, due to the computational difficulties of that time, it was difficult to solve such a problem in order to generate a grasp with the desired properties. Since the mid-90's and up until nowadays though, Grasping research, based on the important theoretical analysis and explorations of the past and making use of state-of-the-art computational, simulational but also mechanical tools and innovations, has become more applied and has approached more efficiently the real world and the physical environment. In particular, a lot of research studies have been devoted to the development of intelligent algorithms and their applications to real, mechanical and complex robot hands. Nowadays, a high level, human-like grasp decision can lead to the appropriate grasp selection and its successful implementation. Therefore, there are almost unlimited opportunities in Grasp Synthesis research, i.e. the research devoted in the successful generation of a grasp. Indeed, there exists a great amount of research devoted to the development of Grasp Synthesis algorithms. Based on the work of P.

Bidaud et al. in [5], we could classify the Grasp Synthesis algorithms in two main categories of approaches: the analytical ones and the empirical ones. By the term analytical approaches, we mean those based on geometric, kinematic and/or dynamic formulations of grasp synthesis problems. On the contrary, by the term empirical approaches, we denot those which avoid the computation of the mathematical and physical models by miming or imitating human strategies.

In the context of this thesis, we have adopted an analytical approach of the Grasping problem. Such an approach requires good knowledge of the system parameters, including both the robotic hand's architecture and the surrounding environment, which is not always easy to be acquired. Besides, the number of the physical, geometrical and mechanical conditions that must be satisfied in order to ensure a successful grasp and task execution are also indicative of the complexity of the computation of such a problem. However, the advantage of this approach is that is closer to the physical environment. Making use of the laws of nature, an analytical algorithm makes use of the laws of nature, taking also into consideration the hardware limitations of the system. This is exactly the philosophy behind the algorithms developed and presented in this document. Fig. 1.4 provides a complete, visualized presentation of the analytical grasp synthesis approach.

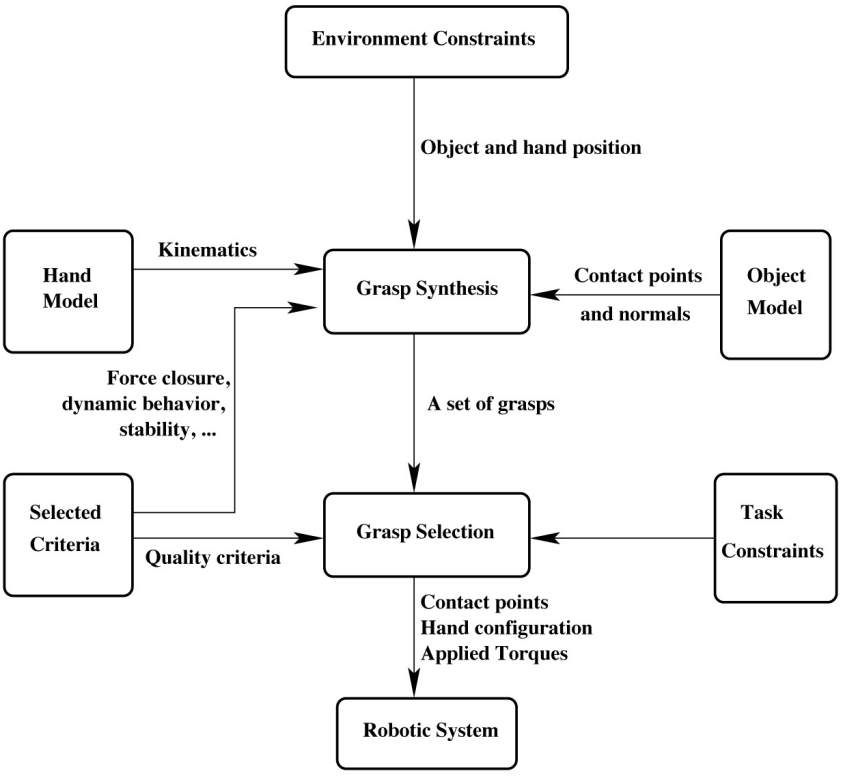

FIGURE 1.4: Analytical approach

1.3 Literature

Over the last decades, there has been a tremendous progress in the field of robotic hands [6]. Simple grippers have been replaced by complex human like hands, built to grasp and manipulate a wide range of every day life objects. However, to perform succesfully, efficient algorithms, that guarantee certain quality criteria concerning the desired grasp properties for the task to be executed, have to be employed. As a result, a lot of research has been conducted in the field of grasp quality, which is defined by metrics that quantify the performance of a grasp. A fundamental and widely accepted quality criterion for a grasp is force closure [7]. It ensures both that the grasped object's weight is compensated as well as that the contact friction constraints are not violated. However, force closure is quite a wide criterion. Therefore and owing to the increasing needs for precise and human like grasps, several other quality measures have been presented. Ferrari and Canny in [8] addressed the problem of minimizing contact forces and proposed two different optimality criteria. Based on [8], Miller and Allen in [9], implemented 3d grasp quality computations for the Barrett and the DLR robotic hands. Moreover, Mishra, in [10] compared various metrics and presented a corresponding mathematical analysis. A useful review on various grasp quality measures can be found in [11]. A lot of grasp synthesis algorithms have been proposed combining different quality measures. Various approaches have been presented both empirical and analytical. The empirical approaches use mainly learning techniques in order to mimic human grasping (as in [12]). On the other hand, the analytical techniques use mathematical formulations considering the kinematics and the dynamics in order to determine optimal grasps regarding certain criteria [5]. In [13], a grasp optimization algorithm with respect to an uncertainty grasp index as well as a task compatibility index is proposed. Particular emphasis has also been devoted to the grasping force optimization (GFO) problem (i.e., the problem of finding the minimal forces that satisfy the force closure sufficient conditions); many algorithms have been proposed in this direction (a complete and thorough overview of grasp synthesis algorithms concerning force optimization but also other metrics and approaches can be found in [5]). The problem of optimizing the maximum external wrench that a multifingered robot hand can withstand is studied in [14]. Finally the force limitations due to hardware and the increasing needs for real time computations have also been taken into consideration in the ongoing research [15]. Another important issue regarding grasp quality is the selection of contact points, which affects severely the force distribution yielded by the aforementioned grasping force optimization algorithms as well as other aspects of grasp quality. Optimality criteria for the selection of contact points were proposed in [16] and [17]. A study on how infinitesimal perturbations of contact points would affect a class of grasp quality functions was presented in [18]. In

[19], it is shown how different contact locations can affect the optimal force distribution with respect to various quality measures.

The main goal of all these studies is to be incorporated as part of an algorithm for planning optimal grasps. In [20] a multi criteria optimization algorithm regarding the fingers ability for force and velocity exertion was presented and was applied specifically for the case of the NASA-JSC robonaut hand, while in [21] a strategy of moving fingers to neighboured joint positions to produce optimal force distribution is proposed.

1.4 Contribution

The contribution of this thesis is based on the:

- Formulation and development of a Grasp Quality optimization algorithm for a multifingered robot hand with fifteen actuated DOFs, such as the DLR/HIT II five fingered robot hand, which is part of the NeuroRobotics Lab equipment
- Development of a methodology that takes into consideration the constraints imposed by the robotic hand and guarantees the stability of the grasp despite potential deviations of the grasping parameters. The presented approach is validated through simulated examples and experimental paradigms. For the grasp implementation an appropriate tactile sensor was used. This work was accepted for publication in the proceedings of the IEEE International Conference on Robotics and Automation (ICRA), Hong Kong, China, 2014
- Utilization of the concept of Q distance towards deriving task oriented optimal grasps

1.5 Thesis structure

Below the organization of the particular thesis is described:

- In Chapter 2 the basics of grasp analysis are presented. In addition, the force closure property will be deeply explained. These theoretical aspects will be used throughout this thesis
- Chapter 3 includes the presentation of multiple algorithms that yield optimal force closure grasps. Special emphasis is given on the concept of Q distance. In addition, some grasp quality metrics will be reviewed

- Chapter 4 introduces the concept of independent contact regions towards dealing with positioning inaccuracies
- Chapters 5, 6 and 7 present the formulation of optimization schemes that lead to a successful grasp implementation despite a wide range of uncertainties. Task specificity is also addressed
- Chapter 8 concludes the thesis

Chapter 2

Contact modelling and basic properties

This chapter introduces the fundamental modelling techniques for grasp analysis and is based on [22]. The overall model is a coupling of models that define contact behaviour with widely used models of rigid body kinematics.

A mathematical model of grasping must be capable of predicting the behaviour of the hand and object under the various loading conditions that may arise during grasping. Generally, the most desirable behaviour is grasp maintenance in the face of unknown disturbing forces and moments applied to the object. Typically, these disturbances arise from inertia forces which become appreciable during high-speed manipulation or applied forces such as those due to gravity. Grasp maintenance means that the contact forces applied by the hand are such that they prevent contact separation and unwanted contact sliding. The special class of grasps that can be maintained for every possible disturbing load is known as closure grasps.

Special emphasis will be placed on explaining the fundamentals of force closure. In brief, this property ensures grasp maintenance.

2.1 Definitions and main quantities

Assume that the links of the hand and the object are rigid and that there is a unique, well-defined tangent plane at each contact point. Let $\{N\}$ represent a conveniently chosen inertial frame fixed in the workspace. The frame $\{B\}$ is fixed to the object with its origin defined relative to $\{N\}$ by the vector $p \in \mathbb{R}^3$, where $\mathbb{R}^3$ denotes three dimensional Euclidean space. A convenient choice for p is the center of mass of the

object. The position of contact point i in $\{N\}$ is defined by the vector $c_i \in \mathbb{R}^3$. At contact point i, we define a frame $\{C\}_i$, with axes $\{\hat{n}_i\ \hat{t}_i\ \hat{o}_i\}$ ($\{C\}_i$ is shown in exploded view in Fig. 2.1). The unit vector $\hat{n}_i$ is normal to the contact tangent plane, and is directed towards the object. The other two unit vectors are orthogonal and lie in the tangent plane of the contact. Let the joints be numbered from 1 to n_q. Denote by $q = [q_1 \dots q_{n_q}]^T \in \mathbb{R}^{n_q}$ the vector of joint displacements, where the superscript $()^T$ indicates matrix transposition. Also, let $\tau = [\tau_1 \dots \tau_{n_q}]^T \in \mathbb{R}^{n_q}$ represent joint loads (forces in prismatic joints and torques in revolute joints). These loads can result from actuator actions, other applied forces, and inertia forces. They could also arise from contacts between the object and hand. However, it will be convenient to separate joint loads into two components: those arising from contacts and those arising from all other sources. Throughout this chapter, noncontact loads will be denoted by τ.

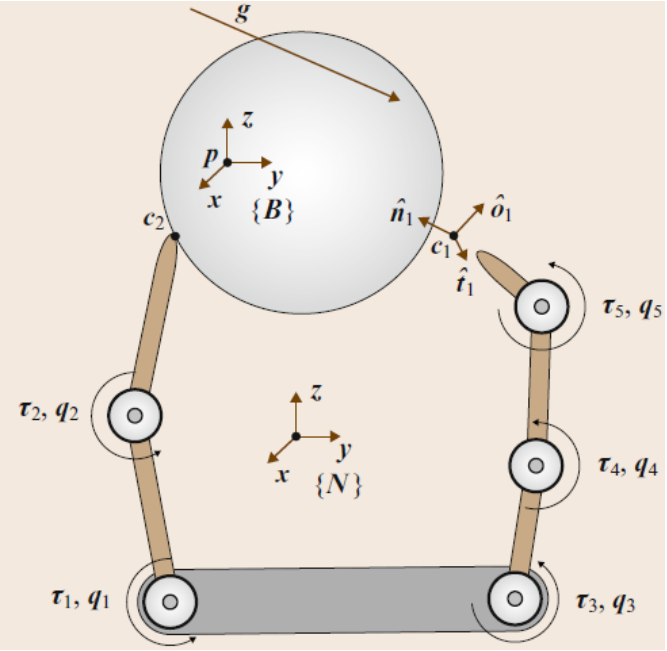

FIGURE 2.1: Main quantities of grasp analysis

Let $u \in \mathbb{R}^{n_u}$ denote the vector describing the position and orientation of $\{B\}$ relative to $\{N\}$. For spatial systems, n_u is three plus the number of parameters used to represent orientation, typically three (for Euler angles) or four (for unit quaternions). Denote by $\nu = [v^T\ \omega^T]^T \in \mathbb{R}^{n_v}$ the twist of the object described in N. It is composed of the translational velocity $v \in \mathbb{R}^3$ of the point p and the angular velocity $\omega \in \mathbb{R}^3$ of the object, both expressed in $\{N\}$. The components of the referred twist represent the velocity of the origin of the new frame and the angular velocity of the body, both expressed in the new frame. An important point is $\dot{u} \neq v$. Instead, these variables are related by the matrix V as:

$$\dot{u} = Vv \tag{2.1}$$

where the matrix $V \in \mathbb{R}^{n_u \times n_v}$ is not generally square but nonetheless satisfies $VV = I$ (I is the identity matrix and the dot over the u implies differentiation with respect to time). Let $f \in \mathbb{R}^3$ be the force applied to the object at the point p and let $m \in \mathbb{R}^3$ be the applied moment. These are combined into the object load, or wrench, vector denoted by $g = [f^T \; m^T] \in \mathbb{R}^{n_v}$, where f and m are expressed in $\{N\}$. Like twists, wrenches can be referred to any convenient frame fixed to the body. One can think of this as translating the line of application of the force until it contains the origin of the new frame, then adjusting the moment component of the wrench to offset the moment induced by moving the line of the force. Last, the force and adjusted moment are expressed in the new frame. As done with the joint loads, the object wrench will be partitioned into two main parts: contact and noncontact wrenches. Throughout this chapter, g will denote the noncontact wrench on the object.

2.2 Grasp Matrix and hand Jacobian

Two matrices are of the utmost importance in grasp analysis: the Grasp Matrix G and the hand Jacobian J. These matrices define the relevant velocity kinematics and force transmission properties of the contacts.

Each contact should be considered as two coincident points: one on the hand and one on the object. The hand Jacobian maps the joint velocities to the twists of the hand expressed in the contact frames, while the transpose of the Grasp Matrix refers the object twist to the contact frames. Finger joint motions induce a rigid-body motion in each link of the hand. It is implicit in the terminology, twists of the hand, that the twist referred to contact i is the twist of the link involved in contact i. Thus these matrices can be derived from the transforms that change the reference frame of a twist.

To derive the Grasp Matrix, let ω^N_{obj} denote the angular velocity of the object expressed in $\{N\}$ and let $v^N_{i,obj}$, also expressed in $\{N\}$, denote the velocity of the point on the object coincident with the origin of $\{C\}_i$. These velocities can be obtained from the object twist referred to $\{N\}$ as:

$$\begin{pmatrix} v^N_{i,obj} \\ \omega^N_{obj} \end{pmatrix} = P_i^T \nu \tag{2.2}$$

where:

$$P_i = \begin{pmatrix} I_{3\times3} & \mathbf{0} \\ S(c_i - p) & I_{3\times3} \end{pmatrix} \tag{2.3}$$

$I_{3\times3}$ is the identity matrix, and $S(c_i - p)$ is the cross-product matrix, that is, given a three-vector $r = [r_x\ r_y\ r_z]^T$, $S(r)$ is defined as:

$$S(r) = \begin{pmatrix} 0 & -r_z & r_y \\ r_z & 0 & -r_x \\ -r_y & r_x & 0 \end{pmatrix}$$

The object twist referred to $\{C\}_i$ is simply the vector on the left-hand side of (2.2) expressed in $\{C\}_i$. Let $R_i = [\hat{n}_i\ \hat{t}_i\ \hat{o}_i] \in \mathbb{R}^{3\times3}$ represent the orientation of the i^{th} contact frame $\{C\}_i$ with respect to the inertial frame (the unit vectors $\hat{n}_i$, $\hat{t}_i$ and $\hat{o}_i$ are expressed in $\{N\}$). Then the object twist referred to $\{C\}_i$ is given as:

$$\nu_{i,obj} = \overline{R}_i^T \begin{pmatrix} v_{i,obj}^N \\ \omega_{obj}^N \end{pmatrix} \tag{2.4}$$

where $\overline{R}_i^T = \text{blockdiag}(R_i, R_i) = \begin{pmatrix} R_i & \mathbf{0} \\ \mathbf{0} & R_i \end{pmatrix} \in \mathbb{R}^{6\times6}$.

Substituting $P_i^T \nu$ from (2.2) into (4.4) yields the partial Grasp Matrix $\tilde{G}_i^T \in \mathbb{R}^{6\times6}$, which maps the object twist from $\{N\}$ to $\{C\}_i$:

$$\nu_{i,obj} = \tilde{G}_i^T \nu \tag{2.5}$$

where

$$\tilde{G}_i^T = \overline{R}_i^T P_i^T \tag{2.6}$$

The hand Jacobian can be derived similarly. Let $\omega_{i,hnd}^N$ be the angular velocity of the link of the hand touching the object at contact i, expressed in $\{N\}$, and define $v_{i,hnd}^N$ as the translational velocity of contact i on the hand, expressed in $\{N\}$. These velocities are related to the joint velocities through the matrix Z_i:

$$\begin{pmatrix} v_{i,hnd}^N \\ \omega_{i,hnd}^N \end{pmatrix} = Z_i \dot{q} \tag{2.7}$$

where $Z_i \in \mathbb{R}^{6\times n_q}$ is defined as:

$$Z_i = \begin{pmatrix} d_{i1} & \dots & d_{in_q} \\ l_{i1} & \dots & l_{in_q} \end{pmatrix} \tag{2.8}$$

with the vectors $d_{ij}, l_{ij} \in \mathbb{R}^3$ defined as:

$$d_{ij} = \begin{cases} \mathbf{0}, & \text{if contact } i \text{ does not affect joint } j \\ \hat{z}_j, & \text{if joint } j \text{ is prismatic} \\ S(c_i - \zeta_j)^T \hat{z}_j, & \text{if joint } j \text{ is revolute} \end{cases}$$

$$l_{ij} = \begin{cases} \mathbf{0}, & \text{if contact } i \text{ does not affect joint } j \\ \mathbf{0}, & \text{if joint } j \text{ is prismatic} \\ \hat{z}_j, & \text{if joint } j \text{ is revolute} \end{cases}$$

where ζ_j is the origin of the coordinate frame associated with the j^{th} joint and $\hat{z}_j$ is the unit vector in the direction of the z-axis in the same frame. Both vectors are expressed in $\{N\}$. These frames may be assigned by any convenient method, for example, the dh method. The $\hat{z}_j$ -axis is the rotational axis for revolute joints and the direction of translation for prismatic joints. An example is illustrated in Fig. **??**.

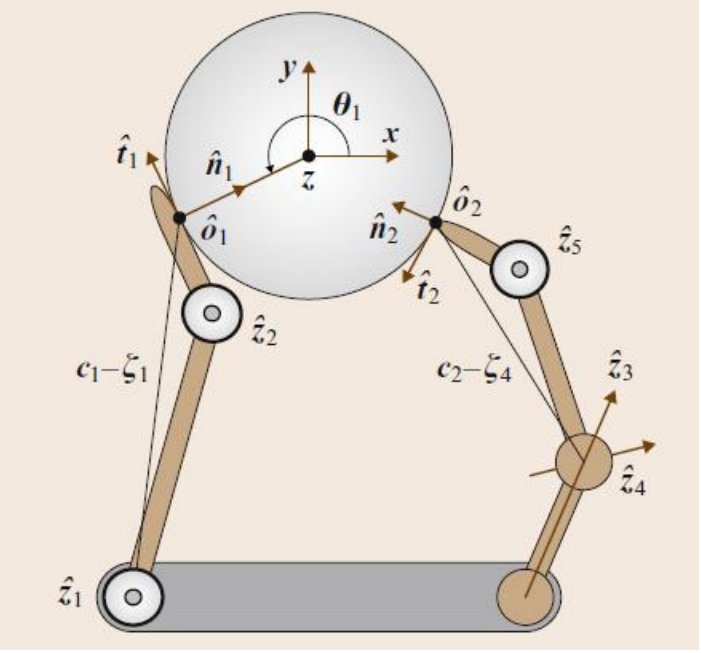

FIGURE 2.2: Example of frames assignment

The final step in referring the hand twists to the contact frames is to change the frame of expression of $\nu^N_{i,hnd}$ and $\omega^N_{i,hnd}$ to $\{C\}_i$

$$\nu_{i,hnd} = \overline{R}_i^T \begin{pmatrix} v^N_{i,hnd} \\ \omega^N_{i,hnd} \end{pmatrix} \tag{2.9}$$

TABLE 2.1: Variables of grasp analysis

notation	**definition**
n_c	number of contacts
n_q	number of joints
n_v	number of degrees of freedom (DoF) of the object
q	joint dislpacements
$\dot{q}$	joint velocities
τ	noncontact joint loads
u	position and orientation of object
ν	twist of object
g	noncontact object wrench
$\{B\}$	frame fixed in object
$\{C\}_i$	contact frame i
$\{N\}$	global frame

Combining (4.7) and (4.5) yields the partial hand Jacobian $\tilde{J}_i \in \mathbb{R}^{6\times n_q}$, which relates the joint velocities to the contact twists on the hand:

$$\nu_{i,hnd} = \tilde{J}_i \dot{q} \tag{2.10}$$

where

$$\tilde{J}_i = \overline{R}_i^T Z_i \tag{2.11}$$

To compact notation, stack all the twists of the hand and object into the vectors $\nu_{c,hnd} \in \mathbb{R}^{6nc}$ and $\nu_{c,obj} \in \mathbb{R}^{6nc}$ as follows:

$$\nu_{c,\xi} = \begin{pmatrix} \nu_{1,\xi}^T & \dots & \nu_{n_c,\xi}^T \end{pmatrix}^T, \quad \xi = (\text{obj,hnd})$$

Now the complete Grasp Matrix $\tilde{G} \in \mathbb{R}^{6\times 6n_c}$ and the complete hand Jacobian $\tilde{J} \in \mathbb{R}^{6n_c\times n_q}$ relate the various velocity quantities as

$$\nu_{c,obj} = \tilde{G}^T \nu \tag{2.12}$$

$$\nu_{c,hnd} = \tilde{J} \dot{q} \tag{2.13}$$

where

$$\tilde{G}^T = \begin{pmatrix} \tilde{G}_1^T \\ \vdots \\ \tilde{G}_{n_c}^T \end{pmatrix} \quad \tilde{J} = \begin{pmatrix} \tilde{J}_1 \\ \vdots \\ \tilde{J}_{n_c} \end{pmatrix} \tag{2.14}$$

The term complete is used to emphasize that all $6n_c$ twist components at the contacts are included in the mapping.

2.3 Contact modelling

The three models of greatest interest in grasp analysis are known as point contact without friction, hard finger, and soft finger. These models select components of the contact twists to transmit between the hand and the object. This is done by equating a subset of the components of the hand and object twist at each contact. The corresponding components of the contact force and moment are also equated, but without regard for the constraints imposed by contact unilaterality and friction models.

2.3.1 Friction model

To proceed, this chapter presents the commonly used Coulombs law. Many applications on robotic manipulation and grasping have been based on this model of friction. More sepcifically, this experimental law states that, for the planar case, the friction force magnitude f_t in the tangent plane at the contact interface is related to the normal force magnitude f_n by $f_t \leq \mu f_n$, where μ is called the friction coefficient. If the contact is sliding, then $f_t = \mu f_n$, and the friction force opposes the direction of motion. The friction force is independent of the speed of sliding.

Often two friction coefficients are defined, a static friction coefficient μ_s and a kinetic (or sliding) friction coefficient μ_k, where $\mu_s \geq \mu_k$. This implies that a larger friction force is available to resist initial motion, but once motion has begun, the resisting force decreases. Many other friction models have been developed with different functional dependencies on factors such as the speed of sliding and the duration of static contact before sliding. All of these are aggregate models of complex microscopic behaviour. For simplicity, the simplest Coulomb friction model with a single friction coefficient μ will be used. This model is reasonable for hard, dry materials. The friction coefficient depends on the two materials in contact, and typically ranges from 0.1 to 1.

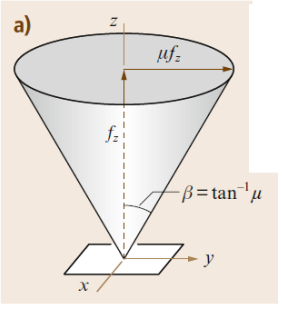

FIGURE 2.3: Friction cone

As shown in Fig. 2.3, this friction law can be interpreted in terms of a friction cone. The set of all forces that can be applied to the object by the supporting line is constrained to be inside this cone. Correspondingly, any force the object applies to the support is inside the negative of the cone. The half-angle of the cone is $\beta = \tan^{-1}\mu$. If the object slips to the left on the support, the force the support applies to it acts on the right edge of the friction cone, with a magnitude determined by the normal force.

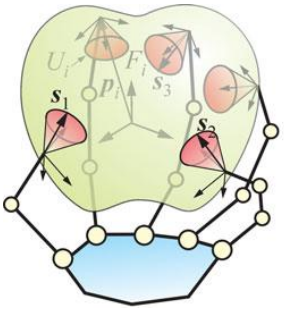

FIGURE 2.4: Illustration of friction cones during grasping

For computational purposes, it is common to approximate circular friction cones as pyramidal cones, as shown in. A more accurate inscribed pyramidal approximation can be used by increasing the number of faces of the pyramid.

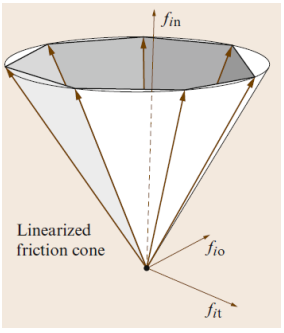

FIGURE 2.5: An inscribed pyramidal approximation to the friction cone

2.3.2 Contact models

- Point contact without friction

The point-contact-without-friction (PwoF) model is used when the contact patch is very small and the surfaces of the hand and object are slippery. With this model, only the normal component of the translational velocity of the contact point on the hand (i.e., the first component of $\nu_{i,hnd}$) is transmitted to the object. The two components of tangential velocity and the three components of angular velocity are not transmitted. Analogously,

the normal component of the contact force is transmitted, but the frictional forces and moments are assumed to be negligible.

- Hard finger

A hard-finger (HF) model is used when there is significant contact friction, but the contact patch is small, so that no appreciable friction moment exists. When this model is applied to a contact, all three translational velocity components of the contact point on the hand (i.e., the first three components of $\nu_{i,hnd}$) and all three components of the contact force are transmitted through the contact. None of the angular velocity components or moment components are transmitted.

- Soft finger

The soft-finger (SF) model is used in situations in which the surface friction and the contact patch are large enough to generate significant friction forces and a friction moment about the contact normal. At a contact where this model is enforced, the three translational velocity components of the contact on the hand and the angular velocity component about the contact normal are transmitted (i.e., the first four components of $\nu_{i,hnd}$). Similarly, all three components of contact force and the normal component of the contact moment are transmitted.

The analysis presented in this thesis is entirely based on the HF model. Thus, the friction model and selection matrices presented below are chosen appropriately.

Define the relative twist of contact i as:

$$\begin{pmatrix} \tilde{J}_i & -\tilde{G}_i^T \end{pmatrix} \begin{pmatrix} \dot{q} \\ \nu \end{pmatrix} = \nu_{i,obj} - \nu_{i,hnd}$$

The HF contact model is defined through the selection matrix $H_i \in \mathbb{R}^{l_i \times 6}$, which selects l_i components of the relative contact twist and sets them to zero (transmitted DoFs)

$$H_i = \begin{pmatrix} I_{3\times 3} & \mathbf{0} \\ \mathbf{0} & \mathbf{0} \end{pmatrix}, \quad H_i(\nu_{i,obj} - \nu_{i,hnd}) = \mathbf{0} \tag{2.15}$$

The contact constraint equations for all n_c contacts can be written in compact form as:

$$H = blockdiag(H_1 \dots H_{n_c}) \in \mathbb{R}^{l \times 6n_c}, \quad H(\nu_{i,obj} - \nu_{i,hnd}) = \mathbf{0} \tag{2.16}$$

and the number of twist components l transmitted through the n_c contacts is given by $l = \sum_{i=1}^{n_c} l_i$. Finally, by substituting (2.12) and (2.13) into (2.16) one obtains:

$$\begin{pmatrix} J & -G^T \end{pmatrix} \begin{pmatrix} \dot{q} \\ \nu \end{pmatrix} = \mathbf{0} \tag{2.17}$$

where $G^T = H\tilde{G}^T$ is the Grasp Matrix and $J = H\tilde{J}$ is the hand Jacobian.

According to the friction coulomb model, each contact force must lie inside its correspoding friction cone in order to avoid slippage. Let us denote by μ the friction coefficient, f_n the normal force component and f_o, f_t the tangential components. In this respect, the friction constraints are formulated as:

$$\sqrt{f_{i_o}^2 + f_{i_t}^2} \leq \mu f_{i_n}, \quad i = 1, ..., n_p \tag{2.18}$$

Linearizing the friction cone by an n_g-sided polyhedral cone, each grasping force can be represented as:

$$f_i = \sum_{j=1}^{n_g} a_{ij} s_{ij}, \quad a_{ij} \geq 0,$$

with $s_{ij} = \begin{pmatrix} 1 \\ cos(2j\pi)/n_g \\ sin(2j\pi)/n_g \end{pmatrix}$, $j = 1, ..., n_g$, denoting the j^{th} edge vector of the linearized friction cone.

2.4 Equilibrium

When the inertia terms are negligible, as occurs during slow motion, the system is said to be quasistatic. In this case, the equation that connects the contact wrenches, the joint loads and the external wrenches is the following:

$$\begin{pmatrix} J^T \\ -G \end{pmatrix} \lambda = \begin{pmatrix} \tau \\ g \end{pmatrix} \tag{2.19}$$

g is the force and moment applied to the object by gravity and other external sources and τ is the vector of actuator actions. The vector λ contains the contact force and moment components transmitted through the contacts and expressed in the contact frames. Specifically, $\lambda = [\lambda_1^T \dots \lambda_{n_c}^T]^T$, where $\lambda_i = H_i[f_{in}\ f_{it}\ f_{io}\ m_{in}\ m_{it}\ m_{io}]^T$. The subscripts indicate one normal (n) and two tangential (t, o) components of contact force

f and moment m. Finally, it is worth noting that $G_i\lambda_i = \tilde{G}_i H_i \lambda_i$ is the wrench applied through contact i, where G_i and H_i are defined in (2.6) and (2.16). The vector λ_i is known as the wrench intensity vector for contact i.

Equation (2.17) is closely related to the kinematic model in (7.11). Specifically, just as J and G^T transmit only selected components of contact twists, J^T and G in (7.11) serve to transmit only the corresponding components of the contact wrenches. Equation (7.11) shows an important alternative view of the Grasp Matrix and the hand Jacobian. G can be thought of as a mapping from the transmitted contact forces and moments to the set wrenches that the hand can apply to the object, while J^T can be thought of as a mapping from the transmitted contact forces and moments to the vector of joint loads.

2.5 Controllable wrenches and twists

In hand design and in grasp and manipulation planning, it is important to know the set of twists that can be imparted to the object by movements of the fingers, and conversely, the conditions under which the hand can prevent all possible motions of the object. The dual view is that one needs to know the set of wrenches that the hand can apply to the object and under what conditions any wrench in $\mathbb{R}^6$ can be applied through the contacts. This knowledge will be gained by studying the various subspaces associated with G and J. The spaces, shown in Fig. 2.6, are the column spaces and null spaces of G, G^T, J, and J^T. Column space (also known as range) and null space will be denoted by $\Re(\dots)$ and $\mathcal{N}(\dots)$, respectively. The arrows show the propagation of the various velocity and load quantities through the grasping system. For example, in the left part of Fig. 2.6 it is shown how any vector $\dot{q} \in \mathbb{R}^{n_q}$ can be decomposed into a sum of two orthogonal vectors in $\Re(J^T)$ and in $\mathcal{N}(J)$ and how $\dot{q}$ is mapped to $\Re(J)$ by multiplication by J.

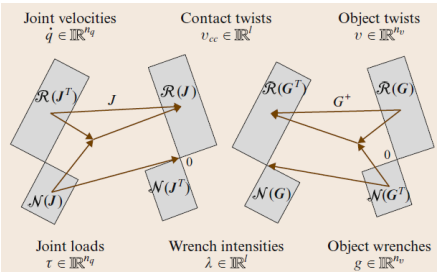

FIGURE 2.6: Linear maps relating the twists and wrenches of a grasping system

Lets us recall the following facts. First, a matrix A maps vectors from $\Re(A^T)$ to $\Re(A)$ in a one-to-one and onto fashion, that is, the map A is a bijection. The generalized inverse A^+ of A is a bijection that maps vectors in the opposite direction. Also, A maps vectors

in $\mathcal{N}(A)$ to zero. Finally, there is no nontrivial vector that A can map into $\mathcal{N}(A^T)$. This implies that, if $\mathcal{N}(G^T)$ is nontrivial, then the hand will not be able to control all degrees of freedom of the object's motion.

2.5.1 Grasp classification

The four null spaces motivate a basic classification of grasping systems. Assuming solutions to (7.11) exist, the following force and velocity equations provide insight into the physical meaning of the various null spaces:

$$\dot{q} = J^+\nu_{cc} + N(J)\alpha \tag{2.20}$$

$$\nu = (G^T)^+\nu_{cc} + N(G^T)\beta \tag{2.21}$$

$$\lambda = -G^+g + N(G)\gamma \tag{2.22}$$

$$\lambda = (J^T)^+\tau + N(J^T)\eta \tag{2.23}$$

In these equations A^+ denotes the generalized inverse, henceforth pseudoinverse, of a matrix A, $N(A)$ denotes a matrix whose columns form a basis for $\mathcal{N}(A)$, and α, β, γ, and η are arbitrary vectors that parameterize the solution sets.

If the null spaces represented in the equations are nontrivial, then it is immediately apparent that many-to-one mappings exist. For instance, consider (2.20). It can be rewritten with ν_{cc} decomposed into components ν_{rs} and ν_{lns} in $\Re(J)$ and $N(J^T)$, respectively, as follows:

$$\dot{q} = J^+(\nu_{rs} + \nu_{lns}) + N(J)\alpha \tag{2.24}$$

Every vector in $N(A^T)$ is orthogonal to every row of A^+. Therefore $J^+\nu_{lns} = 0$. If α and ν_{rs} are fixed in (2.24), then $\dot{q}$ is unique. Thus it is clear that, if $N(J^T)$ is nontrivial, then a subspace of twists of the hand at the contacts will map to a single joint velocity vector.

The equations abpve motivate the following definitions.

- Redundant

A grasping system is said to be redundant if $N(J)$ is nontrivial. Joint velocities $\dot{q}$ in $N(J)$ are referred to as internal hand velocities, since they correspond to finger motions, but do not generate motion of the hand in the constrained directions at the contact

points. If the quasistatic model applies, it can be shown that these motions are not influenced by the motion of the object and vice versa.

- Indeterminate

A grasping system is said to be indeterminate if $N(G^T)$ is nontrivial. Object twists ν in $N(G^T)$ are called internal object twists, since they correspond to motions of the object but do not cause motion of the object in the constrained directions at the contacts. If the static model applies, it can be shown that these twists cannot be controlled by finger motions.

- Graspable

A grasping system is said to be graspable if $N(G)$ is nontrivial. Wrench intensities λ in $N(G)$ are referred to as internal object forces. These wrenches are internal because they do not contribute to the acceleration of the object, i.e., $G\lambda = 0$. Instead, these wrench intensities affect the tightness of the grasp. Thus, internal wrench intensities play a fundamental role in maintaining grasps that rely on friction.

2.5.2 Desirable properties

For a general-purpose grasping system, there are three main desirable properties: control of the object twist ν, control of object wrench g, and control of the internal forces. Control of these quantities implies that the hand can deliver the desired ν and g with specified grip pressure by the appropriate choice of joint velocities and actions. The associated conditions are derived in two steps. First, the structure and configuration of the hand (captured in J) is ignored by assuming that the contact point on the finger can be commanded to move in any direction transmitted by the chosen contact model. An important perspective here is that ν_{cc} is seen as the independent input variable and ν is seen as the output. The dual interpretation is that the actuators can generate any contact force and moment in the constrained directions. Similarly, λ is seen as the input and g is seen as the output. The preliminary property of interest under this assumption is whether or not the arrangement and types of contacts on the object (captured in G) are such that a sufficiently dexterous hand could control its fingers so as to impart any twist $\nu \in \mathbb{R}^6$ to the object and, similarly, to apply any wrench $g \in \mathbb{R}^6$ to the object.

- All object twists possible

Given a set of contact locations and types, by observing the map G on the right side of Fig. 2.6, one sees that the achievable object twists are those in $\Re(G)$. Those in $N(G^T)$ could not be achieved by any hand using the given grasp. Therefore, to achieve any object twist, one must have: $N(G^T) = 0$, or equivalently, $\text{rank}(G) = n_v$. Any grasp with three non-collinear hard contacts satisfies this condition.

- All object wrenches possible

This case is the dual of the previous case, so we expect the same condition. From (7.11), one immediately obtains the condition $N(G^T) = 0$, so again one has $\text{rank}(G) = n_v$. To obtain the conditions needed to control the various quantities of interest, the structure of the hand cannot be ignored. Recall that the only achievable contact twists on the hand are in $\Re(J)$, which is not necessarily equal to $\mathbb{R}^l$.

- Control all object twists

It is obvious that, in order to cause any object twist ν by choice of joint velocities $\dot{q}$, one must have $\Re(GJ) = \Re(G)$ and $N(G^T) = 0$. These conditions are equivalent to $\text{rank}(GJ) = \text{rank}(G) = n_v$.

- Control all object wrenches

This property is dual to the previous one. Analysis of (7.11) yields the same conditions: $\text{rank}(GJ) = \text{rank}(G) = n_v$.

- Control all internal forces

Equation (7.11) shows that wrench intensities with no effect on object motion are only those in $N(G)$. In general, not all the internal forces may be actively controlled by joint actions. It has been shown that all internal forces in $N(G)$ are controllable if and only if $N(G) \bigcap N(J^T) = 0$.

2.6 Restraint analysis

The most fundamental requirements in grasping and dexterous manipulation are the abilities to hold an object in equilibrium and control the position and orientation of the grasped object relative to the palm of the hand. The most useful characterizations of grasp restraint are force closure and form closure. These names were in use over 134

years ago in the field of machine design to distinguish between joints that required an external force to maintain contact, and those that did not. For example, some water wheels had a cylindrical axle that was laid in a horizontal semicylindrical groove split on either side of the wheel. During operation, the weight of the wheel acted to close the groove–axle contacts, hence the term force closure. By contrast, if the grooves were replaced by cylindrical holes just long enough to accept the axle, then the contacts would be closed by the geometry (even if the direction of the gravitational force were reversed), hence the term form closure. When applied to grasping, form and force closure have the following interpretations. Assume that a hand grasping an object has its joint angles locked and its palm fixed in space; then the grasp has form closure, or the object is form closed, if it is impossible to move the object, even infinitesimally. Under the same conditions, the grasp has force closure, or the object is force closed, if for any noncontact wrench experienced by the object, contact wrench intensities exist that satisfy (7.11) and are consistent with the constraints imposed by the friction models applicable at the contact points. Notice that all form closure grasps are also force closure grasps. When under form closure, the object cannot move at force closure over the other three degrees of freedom all, regardless of the noncontact wrench. Therefore, the hand maintains the object in equilibrium for any external wrench, which is the force closure requirement. Roughly speaking, form closure occurs when the palm and fingers wrap around the object forming a cage with no wiggle room. This kind of grasp is also called a power grasp. However, force closure is possible with fewer contacts but in this case force closure requires the ability to control internal forces. It is also possible for a grasp to have partial form closure, indicating that only a subset of the possible degrees of freedom are restrained by form closure. The force closure property is utilized throughout this thesis; thus, further details will be presented.

2.6.1 Force closure

A grasp has force closure, or is force closed, if the grasp can be maintained in the face of any object wrench. Force closure is similar to form closure, but relaxed to allow friction forces to help balance the object wrench. A benefit of including friction in the analysis is the reduction in the number of contact points needed for closure. A three-dimensional object with six degrees of freedom requires seven contacts for form closure, but for force closure, only three (non-collinear) contacts are needed if they are modeled as hard fingers. Force closure relies on the ability of the hand to squeeze arbitrarily tightly in order to compensate for large applied wrenches that can only be resisted by friction. One common definition of force closure can be stated simply by allowing each contact force to lie in its friction cone. Because this definition does not consider the

hand's ability to control contact forces, this definition will be referred to as frictional form closure. A grasp will be said to have frictional form closure if and only if the following conditions are satisfied:

$$\begin{pmatrix} G\lambda = -g \\ \forall g \in \mathbb{R}^{n_v} \\ \lambda \in \mathcal{F} \end{pmatrix}$$

where $\mathcal{F}$ is the composite friction cone. Letting Int($\mathcal{F}$) denote the interior of the composite friction cone, it can be deduced that a grasp has frictional form closure if and only if the following conditions are satisfied:

$$\begin{pmatrix} \text{rank}G = n_v \\ \exists\ \lambda \text{ such that } G\lambda = 0 \\ \lambda \in \text{Int}(\mathcal{F}) \end{pmatrix}$$

These conditions define force closure. The force closure definition adopted here is stricter than frictional form closure; it additionally requires that the hand be able to control the internal object forces.

In addition, a grasp has force closure if and only if rank(G) = n_v, $N(G) \bigcap N(J^T) = 0$ and there exists λ such that $G\lambda = 0$ and $\lambda \in$ Int($\mathcal{F}$). If the rank test passes, then one must still find λ satisfying the remaining three conditions. Of these, the null space intersection test can be performed easily by linear programming techniques, but the friction cone constraint is quadratic, and thus forces one to use nonlinear programming techniques.

Chapter 3

Optimal force closure grasps - Quality measures

In this chapter, multiple methodologies are explained towards deriving optimal grasps. In the first section optimal force closure grasps are studied and the concept of Q distance is considered. Furthermore, quality measures found in the literature that are used to quantify quality and produce optimal configurations are explained.

3.1 Synthesis of Force-Closure grasps based on Q Distance

Here, the concept of Q distance is presented [23]. With some mild and realistic assumptions, the proposed test criterion is differentiable almost everywhere and its derivative can be calculated exactly. On this basis, an algorithm for planning force-closure grasps is presented, which is implemented in the grasp configuration space. The algorithm is generally applicable to planning optimal force-closure grasps on objects with curved surfaces. In brief, the major advantages of the particular quantitative measure lie in the fact that: i)it is differentiable, ii)an optimization problem can be formulated including the kinematic constraints of the robotic hand, iii)it allows the computation of task oriented optimal grasps.

3.1.1 Q^+ distance

Given a compact convex set $Q \subset \mathbb{R}^m$ that contains the origin (i.e., $\mathbf{0} \in \text{int}(Q)$) and any point $\mathbf{a} \in \mathbb{R}^m$, the gauge function of Q is defined as:

$$g_Q(\mathbf{a}) = \left\{ \inf \gamma \mid \mathbf{a} \in \gamma Q, \gamma > 0 \right\}$$

For any $\mathbf{a}, \mathbf{a}' \in \mathbb{R}^m$ and $a > 0$, the gauge function has the following properties: i)$g_Q(\mathbf{a}) \geq 0$; ii)$g_Q(\mathbf{a}) = 0$ if and only if $\mathbf{a} = 0$; iii)$g_Q(\mathbf{a} + \mathbf{a}') \leq g_Q(\mathbf{a}) + g_Q(\mathbf{a}')$; and iv)$g_Q(a\mathbf{a}) = ag_Q(\mathbf{a})$. In addition, if Q is symmetric with respect to the origin of the reference frame (i.e., $Q = -Q$), then v)$g_Q(\mathbf{a}) = g_Q(-\mathbf{a})$. The above properties imply that $g_Q : \mathbb{R}^m \to \mathbb{R}^+$ is a norm in $\mathbb{R}^m$. In the general case, the gauge function may be considered as a pseudonorm, since Q is not necessarily a symmetric set. Hereafter, the gauge function $g_Q(\cdot)$ is denoted by $||\cdot||_Q$, and call it the Q norm. Naturally, the origin-centered sphere in terms of $||\cdot||_Q$, or concisely, the $||\cdot||_Q$ sphere, is defined by $S_Q = \rho Q = \left\{\mathbf{a} \in \mathbb{R}^m \mid g_Q(\mathbf{a}) \leq \rho\right\}$, where $\rho \geq 0$ is the radius of the sphere. In this light, the Q norm is defined in such a way that the unit sphere is determined at first as $S_Q(1) = Q$, from which the $||\cdot||_Q$ norm is induced. In particular, if Q is the unit L_2 sphere, then $||\cdot||_Q$ is just the same as the commonly used L_2 norm. However, since Q can be selected as any compact convex set satisfying $\mathbf{0} \in \text{int}(Q)$, e.g., it is restrained to be a polyhedral set in the sequel, Q may differ significantly from the L_2 norm. Based on the concept of the Q norm, the Q^+ distance will be defined.

Let $\mathbf{p} \in \mathbb{R}^m$ and $A \subset \mathbb{R}^m$ be a point and a convex polyhedron, respectively. The Q^+ distance from $\mathbf{p}$ to A is defined by:

$$d_Q^+(\mathbf{p}, A) = \min ||\mathbf{a} - \mathbf{p}||_Q$$

The concept of Q^+ distance can be directly generalized to two convex polyhedra, P and A, as $d_Q^+(P, A) = \min ||\mathbf{a} - \mathbf{p}||_Q, \mathbf{a} \in A, \mathbf{p} \in P$.

In the sequel, the procedure of computing the Q^+ distance is presented. Q is restrained to be a polyhedral set, which is also specified by the convex hull of its vertices $\mathbf{q}_k$. From the definition of the Q^+ distance, it can be deduced that $d_Q^+(\mathbf{p}, A)$ has the following geometric interpretation. It is the radius of the smallest $||\cdot||_Q$ sphere that is in contact with $A - \{\mathbf{p}\}$. The above observation implies that $d_Q^+(\mathbf{p}, A)$ can be calculated by minimizing ρ subject to the constraint $S_Q \bigcap A - \{\mathbf{p}\} \neq \oslash$. Since:

$$S_Q = \rho Q = \textstyle\sum_{k=1}^K \rho_k \mathbf{q}_k | \sum_{k=1}^K \rho_k = \rho, \rho_k \geq 0$$

$$A - \{\mathbf{p}\} = \textstyle\sum_{i=1}^N a_i \mathbf{a}_i | \sum_{i=1}^N a_i = 1, a_i \geq 0$$

the constraint $S_Q \bigcap A - \{\mathbf{p}\} \neq \oslash$ can be represented by a set of linear equations with nonnegative coefficients, and correspondingly, $d_Q^+(\mathbf{p}, A)$ is formulated as:

$$d_Q^+(p, A) = \min \sum_{k=1}^K \rho_k \tag{3.1}$$

$$\text{s.t.} \left\{ \begin{array}{c} \sum_{k=1}^{K} \rho_k q_k = \sum_{i=1}^{N} \alpha_i \mathrm{a}_i - p \\ \sum_{i=1}^{N} \alpha_i = 1 \\ \rho_k, \alpha_i \geq 0 \end{array} \right\}$$

The linear programs above can be solved using the simplex method. Assuming that $\Phi^* = [\rho_1^*, \ldots, \rho_K^*, a_1^*, \ldots, a_N^*]$ denotes the optimal solution vector, the differentiability of Q^+ distance will be presented below.

Let $\mathcal{B}$ and $\mathcal{B}^+$ be the set of basic variables and the set of strictly positive basic variables in Φ^*, respectively. Notice that the linear programming formulation involves m+1 equality constraints and $\mathcal{B}^+ \subset \mathcal{B}$, we have $|\mathcal{B}| = m + 1$ and $|\mathcal{B}^+| \leq m + 1$, where $|\mathcal{B}|$ and $|\mathcal{B}^+|$ denote the cardinal numbers of $\mathcal{B}$ and $\mathcal{B}^+$ respectively. In what follows, $\mathcal{B}^+$ is denoted by $\mathcal{B}^+ = [\rho_{k_1}^*, \ldots, \rho_{k_r}^*, a_{i_1}^*, \ldots, a_{i_s}^*]$. Obviously, we have r+s=$|\mathcal{B}^+|$. Note that, as the optimal solution to the linear program, Φ^* has to satisfy the constraints of (3.1). Therefore, the following linear equations are derived:

$$\left\{ \begin{array}{c} d_Q^+(p, A) = \sum_{j=1}^{r} \rho_{k_j}^* \\ \sum_{j=1}^{r} \rho_{k_j}^* q_{k_j} = \sum_{l=1}^{s} \alpha_{i_l}^* \mathrm{a}_{i_l} - p \\ \sum_{l=1}^{s} \alpha_{i_l}^* = 1 \end{array} \right\} \tag{3.2}$$

As described above, $d_Q^+(p, A)$ can be interpreted as the radius of the smallest origin-centered $|| \cdot ||_Q$ sphere that is in contact with $A - \{\mathbf{p}\}$. Generally, whether or not $d_Q^+(p, A)$ is differentiable is determined by the geometric nature of the contact of the above two sets. In practice, the geometric nature of the contact can be identified by examining the optimal solution vector Φ^* of the linear program (3.1). The following sufficient conditions for the differentiability of $d_Q^+(p, A)$ are derived:

- $d_Q^+(p, A) > 0$
- The linear programming problem (3.1) has the unique optimum
- $|\mathcal{B}^+| = m + 1$

The conditions above guarantee that the contact between $d_Q^+(p, A)Q$ and $A - \{\mathbf{p}\}$ is generic, which is explained as follows. Assume that the above sufficient conditions are

satisfied; then one has r+s=$|\mathcal{B}^+| = m + 1$. Introduce the following notations:

$$F_1 = d_Q^+(p, A)\mathbf{co}(q_{k_1}^*, \ldots, q_{k_r}^*)$$

$$F_2 = \mathbf{co}(\mathrm{a}_{i_1}^*, \ldots, \mathrm{a}_{i_s}^*) - \{\mathbf{p}\}$$

F_1 and F_2 specify an (r-1) dimensional boundary feature of $d_Q^+(p, A)Q$ and an (s-1) dimensional boundary feature of $A - \{\mathbf{p}\}$ respectively. As stated previously, Φ^* is the unique optimal solution to (3.1), which implies that $d_Q^+(p, A)Q$ and $A - \{\mathbf{p}\}$ contact at a single point. Denote the contact point by h; obviously, one has $h \in F_1 \bigcap F_2$. In other words, F_1 and F_2 are the two boundary features of $d_Q^+(p, A)Q$ and $A - \{\mathbf{p}\}$ that are in contact with each other. From the definition of F_1 and F_2, it is easy to realize that dim(F_1)+dim(F_2)=$|\mathcal{B}^+| - 2 = m - 1$. This implies that the contacting feature pair F_1-F_2 is either edge-edge or vertex-facet. Such types of contact are referred to as the generic contact. An important character of the generic contact is that the state of contact is invariant with the infinitesimal motions and/or deformations of the polyhedra that do not cause the breakage of the contact. In other words, the infinitesimal motions and/or deformations of the polyhedra do not change the uniqueness of the contact point and the feature pair in contact. The concept of generic contact can be generalized to the m-dimensional case, and thus, the conditions above imply that the contact between $d_Q^+(p, A)Q$ and $A - \{\mathbf{p}\}$ is generic, which guarantees the differentiability of $d_Q^+(p, A)$. Hereafter, it is assumed that the vertices of A are variables and their coordinate vectors are represented by a set of smooth functions $\mathbf{a}_i(u)$, where u is the vector of real parameters. Accordingly, denote A by $A(u)$, the optimal solution vector of the linear programming formulation by $\Phi^*(u)$, the set of strictly positive basic variables in $\Phi^*(u)$ by $\mathcal{B}^+(u) = [\rho_{k_1}^*(u), \ldots, \rho_{k_r}^*(u), a_{i_1}^*(u), \ldots, a_{i_s}^*(u)]$, and the distance from p to $A(u)$ by $d_Q^+(u)$ respectively. Apparently, all of them are dependent on u. Suppose that u undergoes an infinitesimal change to u+δ. It results in an infinitesimal deformation of $A(u)$, and, hence, an infinitesimal increment on the value of $d_Q^+(u)$ (because of the Lipschitz continuity). If the aforementioned conditions are satisfied, then δ does not change the state of the contact. Thus, (4.2) holds in a neighborhood of u. By representing the quantities in (4.2) as the functions of u, the particular set of equations can be rewritten as:

$$\left\{ \begin{array}{c} d_Q^+(u) = \sum_{j=1}^{r} \rho_{k_j}^*(u) \\ \sum_{j=1}^{r} \rho_{k_j}^*(u) q_{k_j} = \sum_{l=1}^{s} \alpha_{i_l}^*(u) \mathrm{a}_{i_l}(u) - p \\ \sum_{l=1}^{s} \alpha_{i_l}^*(u) = 1 \end{array} \right\} \tag{3.3}$$

The formula for the derivative of $d_Q^+(u)$ can be derived by differentiating (4.3). Thus, by letting u_τ be a single element of u, the partial derivative of $d_Q^+(u)$ with respect to u_τ is determined by:

$$\frac{\partial d_Q^+(u)}{\partial u_\tau} = \Big(\sum_{j=1}^{r} e_j^m\Big) D_1(u)^{-1} \sum_{l=1}^{s} a_{i_l}^*(u) \frac{\partial \mathrm{a}_{i_l}(u)}{\partial u_\tau} \tag{3.4}$$

where $D_1(u) = [q_{k_1}, \ldots, q_{k_r}, \mathrm{a}_{i_s} - \mathrm{a}_{i_1}, \ldots, \mathrm{a}_{i_s} - \mathrm{a}_{i_{s-1}}]$ and e_j^m is the j^{th} row of the m×m identity matrix.

3.1.2 Methodology for grasp planning

Assume that a robotic hand grasps an object with n_p hard contacts. As explained in the previous chapter all force components are transmitted through the contacts. According to the friction coulomb model, each of the n_p forces must lie inside its correspoding friction cone in order to avoid slippage. Let us denote by μ the friction coefficient, f_n the normal force component and f_o, f_t the tangential components. In this respect, the friction constraints are formulated as:

$$\sqrt{f_{i_o}^2 + f_{i_t}^2} \leq \mu f_{i_n}, \quad i = 1, ..., n_p \tag{3.5}$$

Linearizing the friction cone by an n_g-sided polyhedral cone, each grasping force can be represented as:

$$f_i = \sum_{j=1}^{n_g} a_{ij} s_{ij}, \quad a_{ij} \geq 0,$$

with s_{ij} denoting the j^{th} edge vector of the linearized friction cone. Hence, the wrench produced by f_i is given by:

$$w_i = \begin{pmatrix} f_i \\ f_i \times p_i \end{pmatrix} = \sum_{j=1}^{n_g} a_{ij} \begin{pmatrix} s_{ij} \\ s_{ij} \times p_i \end{pmatrix}$$

The vectors $w_{ij} = \begin{pmatrix} s_{ij} \\ s_{ij} \times p_i \end{pmatrix} \in \Re^6$ define the primitive wrenches (i.e., the wrench generated by a force along the j^{th} edge of the linearized friction cone) where p_i represents the position of i^{th} contact point with respect to the object coordinate frame.

In the previous chapter multiple definitions were given for the force closure property; certain criteria must be satisfied in order for the grasp configuration to achieve force

closure. Here, an additional condition will be presented. More specifically, it has been shown that he grasp is force closured if and only if the primitive wrenches positively span the entire wrench space, or equivalently the origin of the wrench space lies strictly inside the convex hull of the primitive wrenches (i.e., $\mathbf{0} \in \text{int } [\mathbf{co}(w_{11}, w_{12}, ..., w_{n_p n_g})]$).

Assume that W contains the primitive wrenches of the grasp configuration. According to the definition of the Q^+ distance, it is easy to prove that if $d_Q^+(\mathbf{0}, \mathbf{co}(W)) = 0$ and only if $\mathbf{0} \in \text{int } [\mathbf{co}(w_{11}, w_{12}, ..., w_{n_p n_g})]$). However, $d_Q^+(\mathbf{0}, \mathbf{co}(W)) = 0$ does not imply $\mathbf{0} \in \text{int } [\mathbf{co}(w_{11}, w_{12}, ..., w_{n_p n_g})]$). Therefore, $d_Q^+(\mathbf{0}, \mathbf{co}(W)) = 0$ is a necessary condition for the force-closure property. It can be easily deduced that a sufficient condition for the force-closure property is desired. For this purpose, the concept of Q^- distance is introduced.

3.1.3 Q^- distance

Assume that $\mathbf{p}$ and A are a point and a convex polyhedron respectively in $\mathbb{R}^m$, so that $\mathbf{p} \in A$. Let ∂A denote the boundary set of A. The Q^- distance of $\mathbf{p}$ and A is defined by:

$$d_Q^-(\mathbf{p}, A) = -\min ||\mathbf{a} - \mathbf{p}||_Q, \ \mathbf{a} \in \partial A \tag{3.6}$$

Obviously, $d_Q^- \leq 0$. In addition, a nonconvex constraint $\mathbf{a} \in \partial A$ is used. The nonconvexity makes it difficult to solve (4.5) directly, and hence, some alternative approach is desired for the calculation of d_Q^-. To this end, the following equivalent definition is presented:

$$d_Q^-(\mathbf{p}, A) = \Big\{ -\max \rho | S_Q = \rho Q \subset A - \{\mathbf{p}\} \Big\} = \Big\{ \min -\rho | S_Q = \rho Q \subset A - \{\mathbf{p}\} \Big\} \tag{3.7}$$

From (4.6), the following geometric interpretation of $|d_Q^-(\mathbf{p}, A)|$ is obtained: it is the radius of the largest $||\cdot||_Q$ sphere contained in $A - \{\mathbf{p}\}$. Note that $\rho Q \subset A - \{\mathbf{p}\}$ is equivalent to $\rho q_k \in A - \{\mathbf{p}\}$, $\forall k$. (4.6) can be represented as a set of linear programs as follows:

$$d_Q^-(k) = \min -\rho$$

$$\text{s.t.} \left\{ \begin{array}{c} \rho q_k = \sum_{i=1}^{N} \alpha_i \mathrm{a}_i - p \\ \sum_{i=1}^{N} \alpha_i = 1 \\ \alpha_i, \rho \geq 0 \end{array} \right\}$$

$$d_Q^-(p, A) = \max_{k=1,...,K} d_Q^-(k) \tag{3.8}$$

By following a similar approach as for d_Q^+, the partial derivative of d_Q^- with respect to u can be calculated as:

$$\frac{\partial d_Q^-(u)}{\partial u_\tau} = e_1^m D_2(u)^{-1} \sum_{l=1}^{m} a_{i_l}^*(u) \frac{\partial a_{i_l}(u)}{\partial u_\tau}$$

$$D_2(u) = [-q_k^*, \ldots, \mathbf{a}_{i_m} - \mathbf{a}_{i_1}, \ldots, \mathbf{a}_{i_m} - \mathbf{a}_{i_m-1}]$$

By the definition of the $Q-$ distance it can be deduced that $d_Q^-(\mathbf{0}, \mathbf{co}(W)) < 0$ is equivalent to $\mathbf{0} \in \text{int}[\mathbf{co}(W)]$ and can be interpreted as a sufficient condition for the force closure property. It can interpreted as the amplitude of the largest wrench that the robotic hand can produce on the grasped object in the worst direction, with the contact forces being constrained with $\sum_{i=1}^{n} ||f_{i_n}|| \leq 1$ (f_{i_n} is the normal component of the contact force at p_i). In the above interpretation, the amplitude of the wrench is measured in terms of $||\ ||_Q$. In light of this, not only d_Q provides a qualitative test of the force-closure property, but also quantifies the capability of the grasp in resisting unknown external loads and/or disturbances. Thus, starting from a random grasp configuration, an optimal force closure grasp can be obtained by minimizing:

$$d_Q(\mathbf{0}, \mathbf{co}(W)) = \begin{cases} d_Q^+(\mathbf{0}, \mathbf{co}(W)), & \mathbf{0} \notin \text{int } [\mathbf{co}(W)] \\ d_Q^-(\mathbf{0}, \mathbf{co}(W)), & \mathbf{0} \in \text{int } [\mathbf{co}(W)] \end{cases}$$

3.2 Different approaches for obtaining force closure grasps

Apart from the concept of Q distance other approaches have focused on deriving force closure grasps as well. Some of these approaches will be summarized below.

- Solving a ray shooting problem

In [24], the configuration achieves force closure by using a test in each iteration that implies the solution of a linear programming problem based on the ray-shooting technique. It is able to deal with frictional and frictionless contacts starts with the random selection of n contact points and then iteratively moves the points to reduce the distance between the convex hull of the applied wrenches and the origin of the wrench space. A force closure configuration is guaranteed but the particular approach does not ensure any optimality.

- Geometrical approach

In [25], the procedure to search for force closure grasps has a heuristic nature and is based on the metric of the largest perturbation wrench that the grasp resists, independently of its direction. During this procedure the facet of the corresponding convex hull that limits the grasp quality is identified, and one of its vertices (primitive wrenches associated with a contact point) is iteratively replaced to look for a better grasp. The drawback of this technique is the difficulty surrounding the incorporation of the kinematic constraints of the robotic hand.

3.3 Quality measures

So far, the presented algorithms deal with the search for an optimal force closure grasp. However, the quality of a grasp is not only measured by its ability to resist all posible disturbances. In some cases it may be desired to optimize different quality measures. In this respect, multiple quality measures will be presented that evaluate the goodness of a grasp based either on the position of the contact points or the configuration of the robotic hand. A more detailed description can be found in [11].

- Distance between the centroid of the contact polygon and the center of mass of the object

The effect of inertial and gravitational forces on the grasp is minimized when the distance between the center of mass of the object, CM, and the centroid C of the contact polygon is minimized. This distance is also used as a grasp quality measure:

$$Q = ||CM - C||$$

- Normal directions at the contact points

The sum of the components of the applied forces normal to the object boundary is indicative of the internal forces that the object withstands when an external disturbance is applied. Then, a quality measure is defined as the sum of the modules of the normal components of the applied forces required to achieve an expected demanding wrench:

$$Q = \min \sum f_{in}$$

- Distance to singular configurations

In order to keep redundant arms away from singular configurations, it is desirable to maximize the smallest singular value σ_{min} of the manipulator Jacobian. The same idea is applied to grasps with mechanical hands using the hand-object Jacobian H, which in a singular grasp configuration has at least one of the singular values equal zero. Therefore, by using $\sigma_{min}(H)$ as a quality measure, maximizing the quality is equivalent to choose a grasp configuration far away from a singular one:

$$Q = \sigma_{min}(H)$$

- Volume of the manipulability ellipsoid

The measure $\sigma_{min}(H)$ considers only one singular value of H, which may be similar for two different grasp configurations. In order to consider all the singular values of H, the volume of the manipulability ellipsoid is proposed as quality measure. Let $\sigma_1, \ldots, \sigma_r$ be the singular values of H. The grasp quality (i.e. the volume of the manipulability ellipsoid) is:

$$Q = k\sqrt{det(HH^T)} = k(\sigma_1 \ldots \sigma_r)$$

Chapter 4

Independent contact regions

So far the presented analysis emphasizes on the theoretical aspect of grasping; it has been assumed that all parameters are known. However, parameters often differ from their nominal value during experimental procedures. More specifically, robotic hands can hardly assure that the fingers will precisely touch the object at the computed contact points. In this respect the concept of independent contact regions (ICRs) is introduced to provide robustness to finger positioning errors during an object grasping: a finger contact anywhere inside each of these regions assures a force-closure grasp, despite the exact contact position.

4.1 Grasping Uncertainties

A key influence on force closure is the presence of grasping uncertainties, which are inevitable in practice and can lead to unpredictable, probably undesirable results. For secure application of a force closure grasp, it is necessary to figure out the capability of the grasp to tolerate grasping uncertainties, since the force closure property is not guaranteed.

The force closure property of grasps depends on the contact types. For HF contacts, friction coefficients are uncertain. Tangential friction is very sensitive to the environment. Under vibration, or with oil orwater on the contact surface, the coefficients are liable to diminish. This changes the contact constraints and thus affects the force-closure property.

Often contacts cannot be located exactly in the desired positions and obtaining their actual positions without uncertainty is very difficult, even impossible. Contact position uncertainty can be easily expressed by a position deviation, which occurs initially when

the contact is located and further rises under the influence of the environment. The position deviation alters the Grasp Matrix, so that the feasible resultant wrenches that the grasp can generate are transformed. As shown in [26], the deviation may grow to such an extent that computation of force closure grasps using exact contact positions may be completely unreliable in reality.

The aforementioned uncertainties and their influence are depicted in Fig. 4.1.

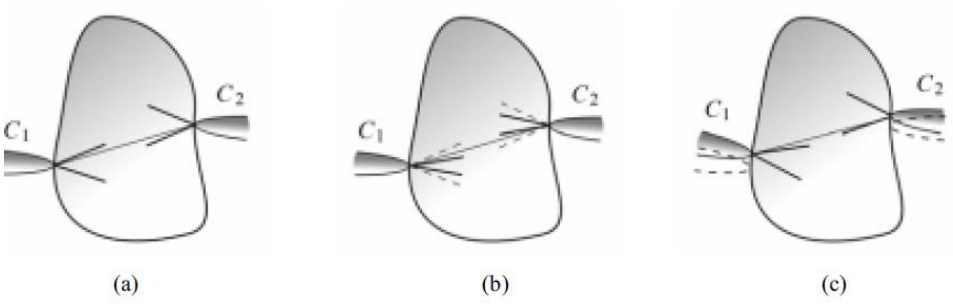

FIGURE 4.1: A planar grasp with two point contacts with friction. (a) The grasp is force closure, as the line connecting the contact points lies inside both friction cones. (b) Compared with (a), the grasp is not force closure any more, owing to the decline of friction coefficients. The dashed lines depict the original friction cones. (c) Compared with (a), the grasp loses the force closure property because of tiny deviations at the contact positions. The dashed curves indicate the original contact positions

Other uncertainties include deviations in the object boundary, stiffness and center of mass as weell as parameters regarding the configuration of the robotic hand. Some of these uncertainties will be tackled with the introduction of the independent contact regions. Deviations of other grasping parameters will be tackled by deriving appropriate contact forces.

4.2 Independent contact regions

4.2.1 Definition

Suppose an n_p-fingered robotic hand grasping a rigid object with n_p point-to-point frictional contacts. The hard finger model is adopted, implying that all force components are transmitted through the contacts. According to the friction coulomb model, each of the n_p forces must lie inside its correspoding friction cone in order to avoid slippage. Let us denote by μ the friction coefficient, f_n the normal force component and f_o, f_t the tangential components. In this respect, the friction constraints are formulated as:

$$\sqrt{f_{i_o}^2 + f_{i_t}^2} \leq \mu f_{i_n}, \quad i = 1, ..., n_p \tag{4.1}$$

Linearizing the friction cone by an n_g-sided polyhedral cone, each grasping force can be represented as:

$$f_i = \sum_{j=1}^{n_g} a_{ij} s_{ij}, \quad a_{ij} \geq 0,$$

with s_{ij} denoting the j^{th} edge vector of the linearized friction cone. Hence, the wrench produced by f_i is given by:

$$w_i = \begin{pmatrix} f_i \\ f_i \times p_i \end{pmatrix} = \sum_{j=1}^{n_g} a_{ij} \begin{pmatrix} s_{ij} \\ s_{ij} \times p_i \end{pmatrix}$$

The vectors $w_{ij} = \begin{pmatrix} s_{ij} \\ s_{ij} \times p_i \end{pmatrix} \in \Re^6$ define the primitive wrenches (i.e., the wrench generated by a force along the j^{th} edge of the linearized friction cone) where p_i represents the position of i^{th} contact point with respect to the object coordinate frame. Without loss of generality the vectors s_{ij} are considered to be normalized. The grasp is force closured if and only if the primitive wrenches positively span the entire wrench space, or equivalently the origin of the wrench space lies strictly inside the convex hull of the primitive wrenches (i.e., $\mathbf{0} \in$ int $[\mathbf{co}(w_{11}, w_{12}, ..., w_{n_p n_g})]$).

Assume that the H-representation of the convex hull is given as (H, K), where H is a matrix containing the inward-pointing unit normals to the bounding hyperplanes and b a vector containing the distances to the origin.By definition, independent contact region i will contain points each of which can replace p_i and still preserve the force closure property. The idea of adding points in $ICRs$ is illustrated in Fig. 4.2. It shows the convex hull $\mathbf{co}(X)$, spanned by vectors x_i containing the origin. By convexity, $\mathbf{co}(X)$ is

fully contained in one of the half-spaces defined by the hyperplane H_f , corresponding to facet f. Facet f is said to belong to the visible region of a point $\hat{x_i}$ if that point lies in the half-space of H_f not including the origin. Let S_i be the intersection of all half-spaces defined by hyperplanes corresponding to facets which contain x_i, so that Si does not contain the origin.

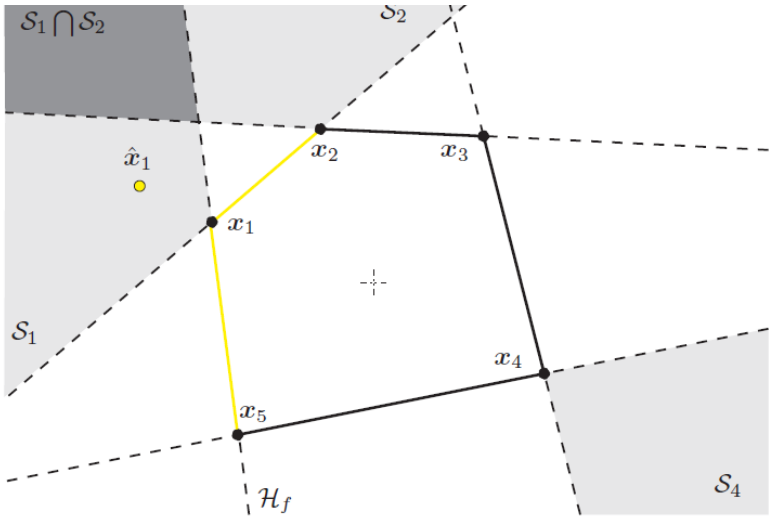

FIGURE 4.2: Visible Region: The yellow facets denote the visible region from the point $\hat{x_1}$ on $\mathbf{co}(X)$. Point x_1 can safely be substituted by $\hat{x_1}$. Points x_1 and x_2 can simultaneously replaced by a point lying in the intersection of search regions $S1$ and $S2$

The following analysis is based on geometric reasoning. Firstly, the convex hull resulting from replacing a vertex x_i with a point $\hat{x_i}$ will fully contain $\mathbf{co}(X)$, if the visible region of x_i on $\mathbf{co}(X)$ is seen by $\hat{x_i}$ as well. This is the case for any $\hat{x_i} \in S_i$. In addition, point $\hat{x_1}$ in Fig. 4.2 can safely substitute x_1 while preserving $\mathbf{co}(X)$ [27].

4.2.2 Computation of $ICRs$

The computation of the independent contact regions ($ICRs$) is infeasible unless the particular grasp configuration achieves force closure [25]. In this respect, the presented analysis, which is based on the work, assumes that the force closure property is guaranteed. To derive a force closure grasp, appropriate algorithms should be applied; certain algorithms were presented in the previous chapter.

To quantify the goodness of a grasp, the considered grasp quality measure, which is one of the most common, is the largest perturbation wrench that the grasp can resist independently of the perturbation direction. This grasp quality is equivalent to the

radius of the largest hypersphere centered on **0** and fully contained in **co**(W) ($W = (w_{11}, w_{12}, ..., w_{n_p n_g})$), i.e., it is the distance from **0** to the closest facet of **co**(W).

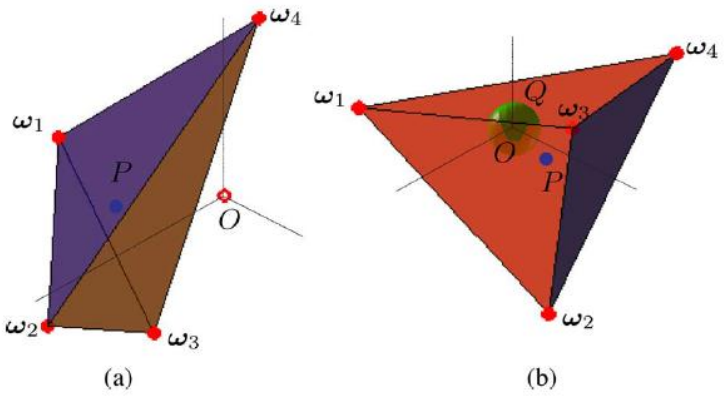

FIGURE 4.3: (a) Non-force closure grasp. Hyperplane formed by $\{w2, w3, w4\}$ leaves P and **0** in different half spaces. (b) force closure grasp. All the supporting hyperplanes of **co**(W) leave P and **0** in the same half space. The radius Q of the largest inscribed sphere indicates the grasp quality

The procedure of computing the $ICRs$ is the following one: Given a starting force closure grasp with quality Q_s, the desired minimum grasp quality $Q_r = \alpha Q_s$ (with $0 < \alpha \leq 1$) for any force closure grasp within the $ICRs$ is selected; when $\alpha \to 0$, the $ICRs$ allow force closure grasps with no lower limit on the grasp quality (note that $Q_r = 0$ is actually a forbidden value as it does not ensure the force closure condition). The larger the Q_r, the smaller the $ICRs$. Therefore, Q_r must be selected as a tradeoff between the desired robustness of potential grasps to external perturbations and the flexibility or error margin in finger positioning on the object surface. Once Q_r is fixed, a set of hyperplanes in the wrench space parallel to the facets of the **co**(W) of the starting grasp and tangent to a hypersphere of radius Q_r is used to determine regions of the wrench space where new wrenches (associated with new contacts) will generate force closure grasps with quality $Q \geq Q_r$. Finally, depending on whether each ICR is constrained to be a continuous region or not, a neighbouring condition of the physical points associated with the new valid wrenches can be imposed.

1. Find a starting force closure grasp with quality Q_s
2. Select the minimum acceptable quality $Q_r = \alpha Q_s$
3. Compute **co**(W)

4. For $i = 1$ to n (i.e., for each contact point p_i), do

   (a) For each facet F_k of $\mathbf{co}(W)$ having at least one vertex w_{ij} , build the hyperplane H_k'' parallel to F_k and at a distance Q_r from the origin $\mathbf{0}$, leaving $\mathbf{0}$ and F_k in different half spaces. Let $H_k''^{+}$ be the open half space such that $w_{ij} \in H_k''^{+}$

   (b) Initialize $ICR_i = (p_i)$

   (c) Label p_i as open

   (d) While there are open points $p_h \in ICR_i$, do

      i. For all the neighboring points p_s of p_h, do: If $\exists$ j such that $\forall$ k $w_{sj} \in H_k''^{+}$, then $ICR_i = ICR_i \bigcap (p_s)$, label p_s as open

      ii. Label p_h as closed

5. Return the ICR_s

The procedure is illustrated in Fig. 4.4 for a hypothetical 2d wrench space; note that due to the geometrical construction, any physical point p_h with a primitive wrench w_{hj} in the region S_i can replace the point p_i of the given initial force closure grasp without losing the force closure property and providing a quality $Q \geq Q_r$. Other examples are illustrated in Fig. 4.4,4.5,4.6.

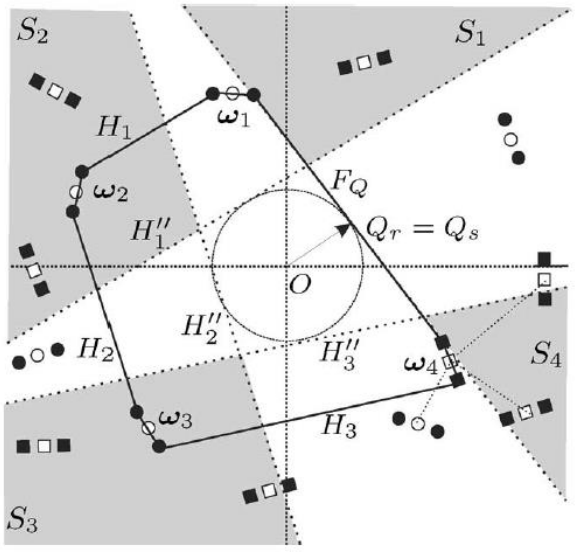

FIGURE 4.4: Search for $ICRs$ ensuring a minimum grasp quality. Search zones S_i for each grasping point are depicted in gray, and the wrenches associated with neighboring points within each ICR are depicted with squares

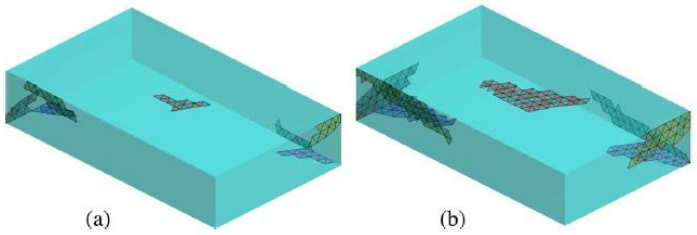

FIGURE 4.5: *ICRs* with a minimum quality of (a)$Q_r = 0.17$, (b) $Q_r = 0.0007$

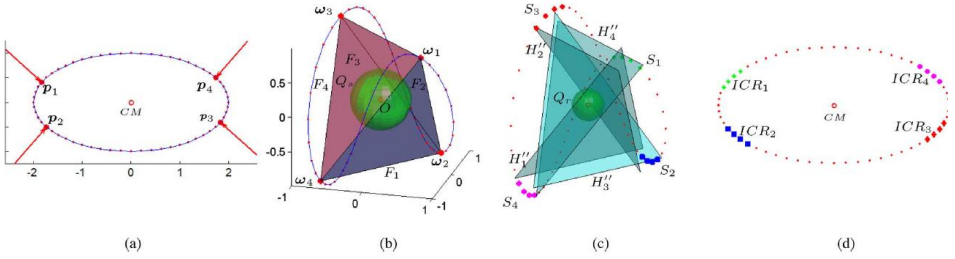

FIGURE 4.6: Search for the *ICRs* for a discretized ellipse. (a) Starting force closure grasp on the ellipse. (b) Starting force closure grasp in the wrench space, with grasp quality $Q_s = 0.43$. (c) Search zones S_i defined by the hyperplanes H_k'' and wrenches within each S_i for Q_r =0.1. (d) *ICRs* on the ellipse

4.3 Influence of uncertainties

Different sources of uncertainty may be present in grasping procedures, for instance, the friction model used in grasp planning, indetermination of the friction coefficients, and

errors in the model of the object that affect the positions of the boundary points as well as the direction normal to the object surface. These uncertainties should be taken into account during the computation of the $ICRs$ [28].

As the material and the surface properties (e.g. roughness, deformations) for the grasped object are, in general, not well known, it is difficult to provide an exact friction coefficient between the fingers and the object. Besides, the coefficients are very sensitive to environment conditions (temperature or vibration, dust, oil or water on the surfaces). In general, these factors tend to diminish the nominal friction coefficient μ_{nom}. The effect of this uncertainty could be modelled as:

$$\mu_{min} = \mu_{nom}/k \tag{4.2}$$

with $k \geq 1$ the reduction coefficient. With the expression provided in (4.2), two different $ICRs$ can be computed for the object: i)$ICRs_{nom}$: nominal $ICRs$, computed for μ_{nom}. This is the ideal case. ii)$ICRs_{min}$: minimal $ICRs$, computed for μ_{min}. Note that diminishing μ may potentially lead to a situation where the force closure property for the starting grasp cannot be guaranteed any longer. If this is the case, then the computation of $ICRs$ will lead to an empty set of $ICRs$. The minimal $ICRs$ allow a force closure grasp despite any variation of μ, i.e. they are the most secure $ICRs$ to grasp the object. If at least one robotic finger is outside its ICR_{min}, then getting a force closure grasp cannot be guaranteed due to friction uncertainty. As an example, Fig. 4.7 shows the computation of the $ICRs_{nom}$ and $ICRs_{min}$ for a parallelepiped, with $\mu = 0.4$. The real $ICRs$ must lie in the ambiguity zone, i.e. somewhere between the $ICRs$ nominal and minimal.

The representation of a real 3d object as a cloud of points or as a triangular mesh could involve several errors due, for instance, to possible locations occluded in the images used to build the model, or to intrinsic errors in the acquisition system. As the grasp quality depends strongly on the location of the contact points and its corresponding normal directions, the effects of geometrical uncertainties should also be considered. These uncertainties should be included in the computation of $ICRs$.

The location p_{ib} of the actual boundary contact point is considered to be inside a closed sphere of radius Δp_i centered at the nominal position p_i of the boundary point, i.e. $p_{ib} = p_i + \alpha \Delta p_i$, with $0 < \alpha < 1$. The primitive wrenches produced at the potential locations of the real contact point are described with:

$$w_{ij} = \begin{pmatrix} s_{ij} \\ s_{ij} \times p_{ib} \end{pmatrix} = \begin{pmatrix} s_{ij} \\ s_{ij} \times p_i \end{pmatrix} + \begin{pmatrix} 0 \\ \alpha \Delta p_i \times s_{ij} \end{pmatrix} \tag{4.3}$$

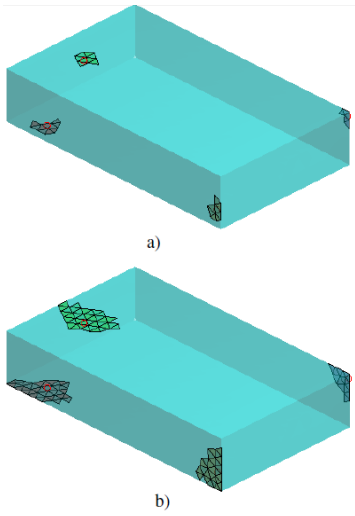

FIGURE 4.7: Independent contact regions on a parallelepiped with $Q_r = 0.04$: a) Minimal $ICRs, \mu_{min} = 0.1$; b) Nominal $ICRs, \mu_{nom} = 0.4$. Note that the higher the friction coefficient, the larger the ICR_i obtained

Thus, the uncertainty in the location of the contact point is a perturbation $\Delta\tau$ affecting only the torque components of the wrench. Note that the magnitude of s_{ij} in (4.3) is 1, so the magnitude of the maximum perturbation in the torque direction is:

$$||\Delta\tau||_{max} = ||\Delta p_i \times s_{ij}|| = ||\Delta p_i|| \tag{4.4}$$

To illustrate the effect of this perturbation in the computation of the $ICRs$, Fig. 4.8 illustrates a hypothetical 2-dimensional wrench space, with the horizontal axis representing the force component f and the vertical axis representing the torque component τ for the wrench. Let a generic hyperplane H_k be described with the equation $e \cdot w = e_0$, where e is the vector normal to the hyperplane. The distance of the hyperplane to the origin is given by:

$$D = |e_0|/||e|| \tag{4.5}$$

Now, let every point of a hyperplane H_k'' be moved by a distance $\Delta\tau$ in the torque direction. A new hyperplane H_k^b is obtained in this way, which takes into account the maximum error in the location of a contact point. The original hyperplane H_k'' is tangent to a hypersphere with radius Q_r; the new hyperplane H_k^b is tangent to a hypershpere with radius R_b given by:

$$R_b = Q_r + \Delta\tau\ e \tag{4.6}$$

Note that this holds true for the 6-dimensional wrench space, as the radius R_b is computed as the original radius plus the projection of the uncertainty $\Delta\tau$ on the vector e

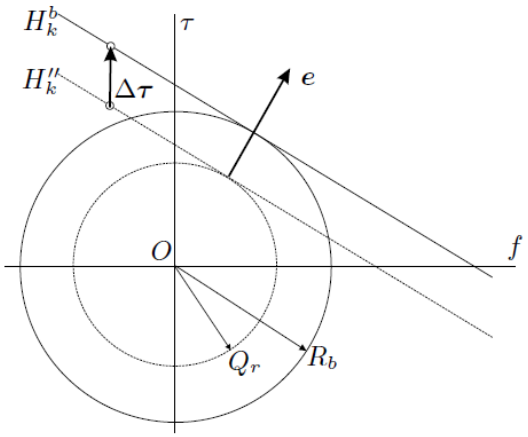

FIGURE 4.8: Uncertainty in the contact location results in a displacement of the hyperplanes defining the search zones

normal to the hyperplane H_k''.

The consideration of uncertainty in the location of the contact points can be taken into account with the computation of the following ICRS: i)$ICRs_{nom}$: nominal $ICRi$ using the nominal position p_i for all the contact points, ii)$ICRs_{min}$: minimal $ICRi$ using the hyperplanes H_k^b parallel to the nominal hyperplanes H_k'' with a distance to the origin given by $R_{b_{min}} = Q_r + \Delta\tau\ e$. Then, the consideration of this uncertainty implies computing the $ICRs$ with a minimum quality R_b larger that the predefined quality Q_r.

Another parameter that may deviate from its nominal value is tirection normal to the object boundary. In order to model this uncertainty, all the potential normal directions are considered to be contained inside a cone with semiangle θ and with its axis along the nominal normal direction. The real friction cone is somewhere between the minimal and maximal cones depicted in Fig. 4.9. Let μ be the friction coefficient (assuming no uncertainty in its determination, or considering μ as a conservative friction coefficient). The friction cones have a semiangle of:

$$\text{minimal} : \theta_{min} = \text{atan}(\mu) - \theta \tag{4.7}$$

$$\text{maximal} : \theta_{max} = \text{atan}(\mu) + \theta \tag{4.8}$$

The influence of the aforementioned uncertainties are illustrated in Fig. 4.10.

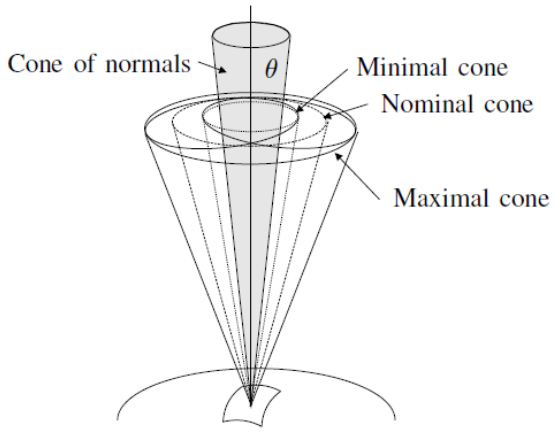

FIGURE 4.9: Uncertainties in the normal direction define a cone of normals containing all the possible normal directions. All the potential friction cones can be found between a minimal and a maximal cone

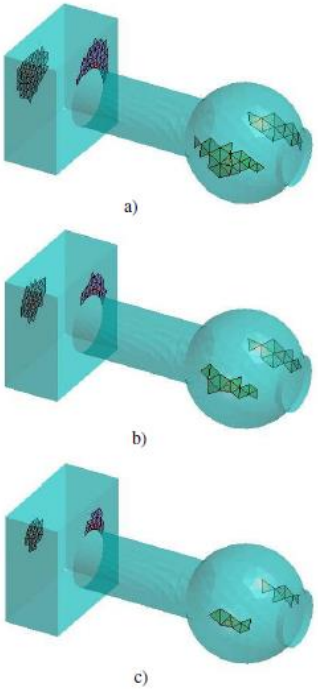

FIGURE 4.10: Independent contact regions: a)Nonimal $ICRs$ (no uncertainty); b)Minimal $ICRs$, (considering uncertainty in the normal direction); c) Minimal $ICRs$ with the combined effect of uncertainty in the normal direction and in the location of the contact points

4.4 Extension of the presented analysis

The authors in [27] made the following suggestions:

- Instead of exclusively checking primitive wrenches for the inclusion in the respective search regions, it was stated that there have to exist possible convex combinations of the primitive wrenches inside all search regions
- If only one search region is defined associated with each p_i (as the intersection of the half spaces all primitive wrenches) smaller or even empty $ICRs$ may be derived
- Instead of measuring the minimum distance between the hyperplanes and $\mathbf{0}$ as the metric, the task wrench space can be incorporated in the analysis. The $ICRs$ contain points that guarantee that the task wrench space will be in the interior of $\mathbf{co}(W)$ (Fig. 4.11)

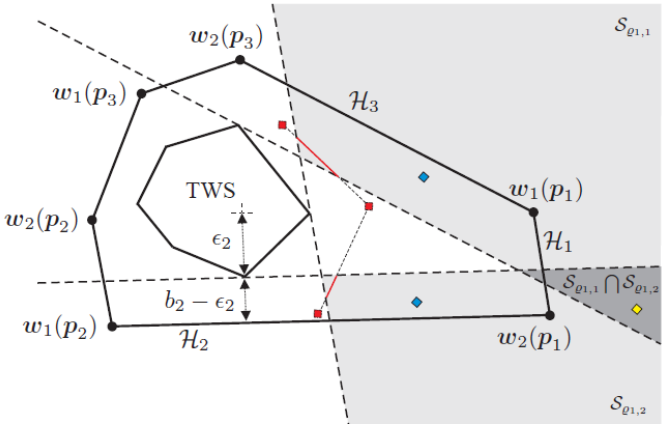

FIGURE 4.11: The red lines denote valid convex combinations of the primitive wrenches, which are shown as red squares. Contact points associated with the primitive wrenches depicted as blue squares, as well as the primitive wrench illustrated as a yellow square also can replace p1 without violating the task wrench space

Chapter 5

Posture selection scheme

The majority of the works on grasping consider both object as well as robot hand parameters to be accurately known and do not take into account the constraints imposed by the robotic hand. In contrast, the proposed methodology [29] is complete in a way that handles the grasping problem under a wide range of uncertainties. Aiming at satisfying the kinematic constraints of the robotic hand, the determination of independent contact regions is incorporated in the posture selection algorithm. In addition, the posture selection scheme yields a configuration that is able to transmit efficiently forces on the contact points. The presented methodology includes the kinematic constraints of the DLR/HIT II robotic hand.

5.1 Problem definition

The software/hardware limitations of a robotic hand together with the uncertainties regarding the object physical properties render the task of precise contact positioning extremely difficult. For example, experimental results in our lab with the DLR/HIT II robot hand, have shown that joint displacement errors occur up to 1.5 degree. In this respect, it is essential to introduce the concept of independent contact regions to the grasp configuration searching algorithm. The initial plan was to formulate the problem so that, given any initial grasp, a robust grasp configuration with respect to positioning errors would be produced. However, the computation of independent contact regions is impossible, unless the particular configuration yields a force closure grasp. Hence, the first step is to generate an efficient force closure grasp, compatible with the kinematic constraints.

In order to lift the object properly, robotic fingers need to apply adequate contact forces without however violating the actuators' limitations. Thus, it is of utmost importance

to adopt a configuration that is capable of exerting satisfactory forces on the object with relatively small joint torque effort. Therefore, starting from the initial force closure grasp, an optimization scheme is formulated in order to find a grasping posture that maximizes the force transmission ratio of the robotic hand and provides robustness against potential contact points deviation. Recent state of the art works, presented in previous chapters, given a force closure grasp, focus on checking which points on the object boundary qualify to be included in the independent contact regions. In the proposed optimization scheme, however, based on the range of the DLR/HIT II joint displacement error, the deviated contact points are constrained to lie inside the independent contact regions. Hence, apart from maximizing the force transmission ratio of the robotic hand, a force closure grasp will be obtained regardless the positioning uncertainties. The output of the algorithms is verified with a simulation study for the case of a robotic hand with the design and limitations of the DLR/HIT II. Nevertheless, it should be noted that the proposed procedure can be applied to every mechanical multi-fingered robotic hand.

5.2 Search for an acceptable force closure grasp

Prior to developing the methodology, the basics of grasping will be given. Consider an n_p-fingered robotic hand with n_q rotational joints in total, grasping a rigid object with n_p point-to-point frictional contacts. The hard finger model is adopted, implying that all force components are transmitted through the contacts. According to the friction coulomb model, each of the n_p forces must lie inside its correspoding friction cone in order to avoid slippage. Let μ denote the friction coefficient, f_n the normal force component and f_o, f_t the tangential components. In this respect, the friction constraints are formulated as:

$$\sqrt{f_{i_o}^2 + f_{i_t}^2} \leq \mu f_{i_n}, \quad i = 1, ..., n_p \tag{5.1}$$

Linearizing the friction cone by an n_g-sided polyhedral cone, each grasping force can be represented as:

$$f_i = \sum_{j=1}^{n_g} a_{ij} s_{ij}, \quad a_{ij} \geq 0,$$

with s_{ij} denoting the j^{th} edge vector of the linearized friction cone. Hence, the wrench produced by f_i is given by:

$$w_i = \begin{pmatrix} f_i \\ f_i \times p_i \end{pmatrix} = \sum_{j=1}^{n_g} a_{ij} \begin{pmatrix} s_{ij} \\ s_{ij} \times p_i \end{pmatrix}$$

The vectors $w_{ij} = \begin{pmatrix} s_{ij} \\ s_{ij} \times p_i \end{pmatrix} \in \Re^6$ define the primitive wrenches (i.e., the wrench generated by a force along the j^{th} edge of the linearized friction cone) where p_i represents the position of i^{th} contact point with respect to the object coordinate frame. Without loss of generality the vectors s_{ij} are considered to be normalized. The grasp is force closured if and only if the primitive wrenches positively span the entire wrench space, or equivalently the origin of the wrench space lies strictly inside the convex hull of the primitive wrenches (i.e., $\mathbf{0} \in \text{int } [\mathbf{co}(w_{11}, w_{12}, ..., w_{n_p n_g})]$).

The grasp selection algorithm is based on the concept of the Q distance for curved objects. In summary, given a polyhedral set $Q \subset \mathbb{R}^6$ that contains the origin (i.e., $\mathbf{0} \in \text{int}[Q]$), a point $p \in \mathbb{R}^6$ and a convex polyhedron $A \subset \mathbb{R}^6$, the Q distance from p to A is calculated as follows:

$-p \notin \text{int}[A]$:	$-p \in \text{int}[A]$:
$d_Q^+(p, A) = \min \sum_{k=1}^{K} \rho_k$ s.t. $\left\{ \begin{array}{c} \sum_{k=1}^{K} \rho_k q_k = \sum_{i=1}^{N} \alpha_i \mathrm{a}_i - p \\ \sum_{i=1}^{N} \alpha_i = 1 \\ \rho_k, \alpha_i \geq 0 \end{array} \right\}$	$d_Q^-(k) = \min -\rho$ s.t. $\left\{ \begin{array}{c} \rho q_k = \sum_{i=1}^{N} \alpha_i \mathrm{a}_i - p \\ \sum_{i=1}^{N} \alpha_i = 1 \\ \alpha_i, \rho \geq 0 \end{array} \right\}$ $d_Q^-(p, A) = \max_{k=1,...,K} d_Q^-(k)$

where q_k $(k = 1, ..., K)$ and a_i $(i = 1, ..., N)$ are the vertices of Q and A respectively. Notice that the aforementioned linear programs can be easily solved using the simplex method. Moreover, the set Q may be chosen to be a simplex in order to reduce the computational complexity.

Assume that W contains the primitive wrenches of the grasp configuration. Then, $d_Q^+(\mathbf{0}, \mathbf{co}(W)) = 0$ represents a necessary condition for the force closure property, while $d_Q^-(\mathbf{0}, \mathbf{co}(W)) < 0$ is equivalent to $\mathbf{0} \in \text{int}[\mathbf{co}(W)]$ and can be interpreted as a sufficient condition. Furthermore, the quantity $|d_Q^-(\mathbf{0}, \mathbf{co}(W))|$ represents the amplitude of the largest wrench the particular grasp can withstand in the worst direction, with $\sum |f_{n_i}| = 1$. Thus, starting from a random grasp configuration, an optimal force closure grasp can be obtained by minimizing:

$$d_Q(\mathbf{0}, \mathbf{co}(W)) = \begin{cases} d_Q^+(\mathbf{0}, \mathbf{co}(W)), & \mathbf{0} \notin \text{int } [\mathbf{co}(W)] \\ d_Q^-(\mathbf{0}, \mathbf{co}(W)), & \mathbf{0} \in \text{int } [\mathbf{co}(W)] \end{cases}$$

Additionally, in case the vertices of W can be represented as smooth functions of a vector l of real parameters $(w_1(l), ..., w_N(l))$, it was proven that the derivatives of d_Q^+ and d_Q^- with respect to l exist and can be computed accurately almost everywhere. In light of this, we formulate our optimization problem by choosing as decision variables the unified vector $v = \begin{bmatrix} q & w \end{bmatrix}^T$, where $q \in \mathbb{R}^{n_q}$ and $w \in \mathbb{R}^6$ denote the joint displacements and wrist position/orientation respectively. We assume that the desired position/orientation of the robotic hand can be implemented by attaching it on a dexterous manipulator. Then, the optimization problem can be formulated as following:

$$\min \; d_Q(\mathbf{0}, \mathbf{co}(W))$$

s.t.

$$q_{min} \leq q \leq q_{max} \tag{5.2}$$

$$fkine(q) \in \partial O \tag{5.3}$$

$$q^j_{abd/add} \leq q^{j+1}_{abd/add} \tag{5.4}$$

$$p' \notin O \tag{5.5}$$

Equation (5.2) describes the joint mechanical limits whereas (5.3) ensures that the fingertips are in contact with the object surface. Furthermore, $q^j_{abd/add}, (j = 1, ..., n_p - 1)$ represents the abduction/adduction degree of freedom of all fingers opposed to the thumb (index, middle, ring, pinky) and equation (5.4) ensures collision avoidance. The next constraint is added in order to avoid penetration between the robotic hand and the object. In particular, p' denotes a set of finite discrete points lying on the robotic hand (the fingertips are excluded). Given an analytical expression of the object boundary, equation (5.5) can be easily expressed as inequality constraints. Henceforth, we shall refer to these constraints using the abbreviation RHC, (*robotic hand constraints*).

Given that the primitive wrenches are expressed as smooth functions, it is possible, through the computation of the manipulator's forward kinematics, to calculate the derivative of the objective function with respect to the decision variables vector v. Thus, computing also the derivatives of the constraints with respect to v, the problem can be solved using a non linear programming algorithm and an optimal force closure grasp configuration can be obtained.

5.3 Dealing with force transmission maximization and positioning inaccuracies

So far the kinematic constraints that need to be satisfied have been taken into account during the grasping posture selection. However, robotic hands are also subjected to joint torque constraints. Thus, it is important to adopt a robot hand configuration that is capable of exerting the required grasping forces on the object with relatively low joint torque effort. Towards this goal, the force transmission ratio r_k and compatibility index c was exploited, which was defined in [30] as:

$$r_k = [u_k^T (J_i J_i^T) u_k]^{-1/2}$$
$$c_i = \sum_{k=1}^{l} r_k^2 = \sum_{k=1}^{l} [u_k^T (J_i J_i^T)_k^u]^{-1}$$

where $u_k, k = 1, ..., l$, denotes the direction of interest regarding the contact forces and J_i denotes the jacobian of the i^{th} finger, $i = 1, ..., n_p$. Since frictional hard contacts have been assumed, each force is restricted to lie inside its corresponding friction cone. Hence, for each contact point the unit vectors u_k are chosen to be aligned with the edges of the linearized friction cone [31]. The compatibility index for the robotic hand is given by:

$$c = \sum_{i=1}^{n_p} w_{f_i} c_i = \sum_{i=1}^{n_p} w_{f_i} \sum_{k=1}^{n_g} [u_k^T (J_i J_i^T) u_k]^{-1}$$

where w_{f_i} are weighting factors, each one for every robotic finger.

Maximization of the compatibility index c yields an optimal posture with respect to the force transmission metric. However, as it was stated previously, different sources may cause deviation between the actual and desired joint positions. Thus, it is important that the robotic hand can grasp the object even if angular displacement errors induce fingertip positioning inaccuracies. For that reason the concept of independent contact regions (ICR) was utilized, adopting, in particular, the approach described in 4.2.2 to determine whether a point on the object boundary qualifies to be a member of an ICR.

In summary, suppose a force closure grasp configuration is given with a quality D. The quality metric considered, is the largest perturbation wrench that can be resisted regardless the perturbation direction and is equal to the distance from $\mathbf{0}$ to the closest facet of the primitive wrenches' convex hull. Each ICR_i consists of a set of discrete points, so that if the fingertips are placed inside the corresponding region, a force closure grasp with a minimum quality D' is obtained. The procedure of computing the $ICRs$

based on the particular method is illustrated in Fig. 5.1a) with a hypothetical 2-d wrench space. In this figure a convex hull of 3 contact points is represented. Each contact point p_i is associated with 4 primitive wrenches w_{ij} and a number of facets F_k, involving at least one vertex w_{ij}. For instance, contact point p_1 is associated with facets F_1 and F_2. H_1', H_2' are the hyperplanes built parallel to F_1, F_2 respectively at a distance D' from $\mathbf{0}$, leaving, also, $\mathbf{0}$ and their corresponding facet at different halfpsaces. A neighbouring point is said to be included in the ICR_1 if at least one of its primitive wrenches lies inside the region $S_1 = \bigcap H_k'^{+}, k = 1, 2$ (we assume that $\mathbf{co}(W) \subseteq H_k^{-}$). The green primitive wrenches depicted in Fig. 5.1a) are associated with contact points inside the ICR_1.

It can be easily deduced that the method proposed in 4.2.2 may be used to determine which neighbouring points are included in the independent contact region, with respect to a minimum desired quality or, equally, a given parallel displacement of the hyperplanes. In this work the range of the joint displacement error is known, hence the deviation of the contact points can be computed. Therefore, instead of checking which points qualify to be inside the $ICRs$, the necessary hyperplane displacements can be determined, so that at least one primitive wrench of each deviated contact point p_s belongs in $\bigcap H_k'^{+}$. Suppose a nominal contact point p_i, the hyperplanes' equations $H_k x = K_k$ associated with the particular point and the deviated contact points $p_s, s = 1, ..., S$ are given. The necessary parallel movement of the hyperplanes for a single contact point can be determined as following:

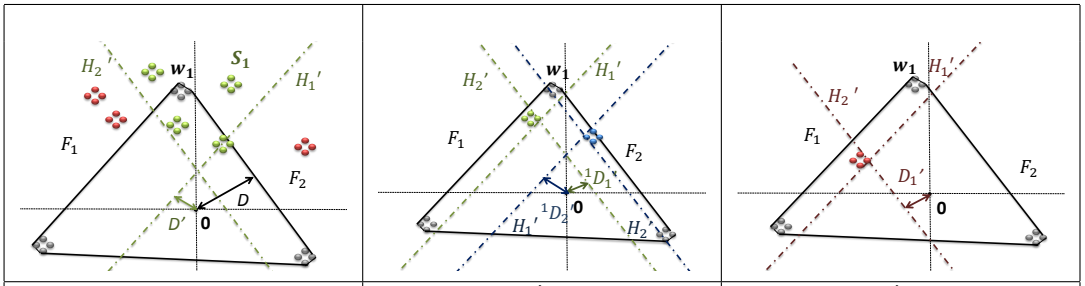

a)ICR determination | b)$D_1' > 0$ | c)$D_1' < 0$

FIGURE 5.1: Independent Contact Regions

- for $s = 1, ..., S$ (for each deviated contact point)
  - for $j = 1, ..., n_g$ (for each primitive wrench of the deviated contact point)
    - for $k = 1, ..., K$ (for each hyperplane H_k having at least one primitive wrench w_{ij})
      - compute the signed distance between the hyperplane H_k and primitive wrench w_{sj}

- build the parallel hyperplane H'_k that involves w_{sj}
- compute the signed distance ${}^iD'_{kj}$ between H'_k and $\mathbf{0}$

- end
- find the required distance ${}^iD'_{j_{min}} = \min({}^iD'_{kj})$ of all hyperplanes H_k from $\mathbf{0}$ so that $w_{sj} \in \bigcap H'^{+}_k$

- end
- find the required distance ${}^iD'_s = \max({}^iD'_{j_{min}})$ of all hyperplanes from $\mathbf{0}$ so that at least one primitive wrench of p_s belongs in $\bigcap H'^{+}_k$

- end

- compute $D'_i = \min({}^iD'_s)$ of all deviated contact points p_s

Notice that the aforementioned distances are computed through vector dot products, rendering the procedure very computationally efficient. The quantity $D' = \min(D'_i)$ of all nominal contact points p_i denotes the maximum distance between $\mathbf{0}$ and all hyperplanes H'_k so that the deviated contact points belong in their corresponding ICR. Furthermore, it is equivalent to the minimum possible quality of the grasp, even if contact points deviation occurs. Last but not least, the signed distance D' must be greater than 0 ($D' > 0$) in order to maintain the force closure property of the grasp. If $D' < 0$ at least one hyperplane H'_k does not contain the origin. The described procedure is illustrated in Fig. 5.1b), c).

Considering the analysis above and keeping as decision variables the unified vector $v = \begin{pmatrix} q & w \end{pmatrix}^T$, the following optimization scheme is formulated that yields a grasp configuration with great force transmission and robustness against positioning inaccuracies:

$$\min \left(w_1 \frac{1}{c} + w_2 \frac{1}{D'} \right)$$

s.t.

$$RHC$$

$$d_Q^-(\mathbf{0}, \mathbf{co}(W)) < 0 \tag{5.6}$$

$$D' > 0 \tag{5.7}$$

It was mentioned earlier that $d_Q^-(\mathbf{0}, \mathbf{co}(W)) < 0$ represents a necessary and sufficient condition for the force closure property. Hence, equation (5.6) constrains the algorithm

to search only force closured grasps. Moreover, equation (5.7) requires the deviated contact points to belong in their corresponding independent contact region. The initial posture provided to the algorithm is the one calculated in the previous section. An optimal configuration with respect to the utilized quality metric results in larger ICRs. In light of this, the optimal grasp configuration generated in the previous section is ideal to initiate the second search algorithm.

Given the object properties, the aforementioned algorithms yielded off-line an optimal posture. For the simulated examples a 2.25 cm-radius, 13 cm-high cylindrical object was considered. Furthermore, due to the robust nature of the analysis, a conservative friction coefficient ($\mu = 0.3$) was selected and the influence of uncertainties related to the friction coefficient and object model in the computation of $ICRs$ was taken into consideration. An initial non force closure grasp and the optimal final grasp (output of the algorithms) are depicted in Fig. 5.2. Based on the joint displacement error of the DLR/HIT II, the maximum contact point deviation on the object was found to be 4 mm. Hence, 4 deviated contact points (presented as red dots in Fig. 5.2) were considered at a distance of 4 mm from their corresponding nominal contact point. For the experimental validation the DLR/HIT II is attached at the end effector of the Mitsubishi PA 10. Note, also, that due to the high accuracy in terms of positioning the Mitsubishi PA10 end effector, errors in the actual wrist position/orientation are neglected. The solution of the optimization schemes was derived using the MATLAB Optimization Toolbox.

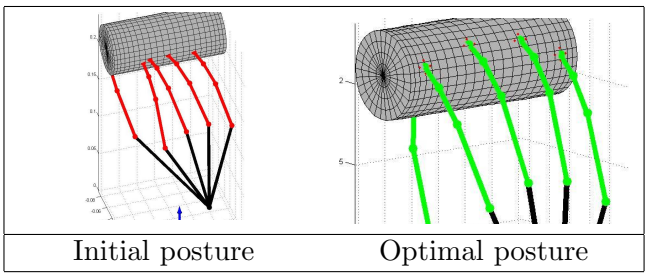

FIGURE 5.2: Simulated postures

Remark 5.1. The quantity D' denotes the minimum quality of the grasp even if contact points deviation occurs. Based on the utilized quality metric, it depends exclusively on the position of the contact points on the surface of the object. On the other hand, the compatibility index c is used so that the resulted configuration of the robotic hand can effectively transform joint torques to contact forces. Considering the above, D' is associated with the transformation of contact forces to object wrenches, while c is connected to the ability of the mechanical system to produce effectively forces to the environment. Hence, the significance of each quality metric can be adjusted by using the weighted factors w_1, w_2.

Chapter 6

Determination of appropriate forces utilizing tactile sensing

Robotic hands are mechanical artifacts subject to joint torque limitations. Thus, apart from choosing a suitable configuration, it is important to be able to perform the grasp with the lowest possible amount of power. Towards this goal, many force optimization algorithms have been proposed [32], [33], [34]. Balancing the external disturbances with relatively small applied forces may prevent the object from deforming and requires low joint torque effort. Nevertheless, uncertainties that may occur during the grasping procedure need to be taken into consideration, so that the robotic hand can lift the object successfully. Most works are designed for precise fingertip positioning on the object and exact knowledge of object parameters, leading, thus, to potential unsuccessful results in real world applications. Inspired by the work in [35], sufficient contact forces are determined that can generate a force closure grasp, even when deviation of contact points and object parameters occurs.

Appropriate tactile devices may contribute to the implementation of dexterous grasping and manipulation tasks, by providing humanoid robots with useful information about geometrical and physical quantities of the objects. In the presented methodology, in order to reduce the magnitude of uncertainty regarding the grasping parameters, valuable information from tactile sensors mounted appropriately on the DLR HIT II was utilized.

To verify the proposed grasping strategy, as well as the methodology presented in the previous chapter, experiments are conducted using the 15 DoF DLR/HIT II attached on the 7 DoF Mitsubishi PA10.

6.1 Introducing the use of appropriate tactile sensors

The tactile sensor used was the off-the-self 4256e Grip sensor designed by Tekscan. This ultra thin (0.15 mm) tactile sensor consists of 320 sensing elements (sensels) and is able to measure the pressure magnitude of each sensel based on piezo-resistive technology. The output of each sensel is divided into 256 increments, and displayed as a value ("raw sum") in the range of 0 to 255 by the software.

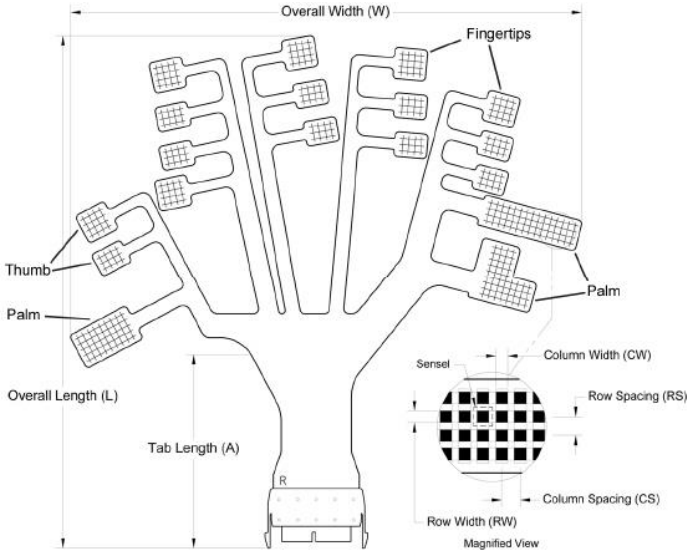

FIGURE 6.1: Tactile sensor

Figures Fig. 6.2 and Fig. 6.3 show how the tactile sensor was mounted on the DLR HIT. Aiming at placing the grip sensor properly, the velcro cyan band and an elastic black tape were used. Initially, the tactile sensor was placed on the DLR HIT so that the active regions could reach the robotic fingertips. Subsequently, the velcro cyan band was used to secure the position of the versatec cuff. Finally, an elastic black tape was used to hold the active regions on the robotic fingertips. to

The active region of each fingertip is a 4x4 array and the sensels' output allows the computation of the center of force, or equally, the contact centroid as:

$$x_{cof} = \frac{\sum_{i=0}^{3} x_i \sum_{j=0}^{3} p_{ij}}{\sum_{i=0}^{3}\sum_{j=0}^{3} p_{ij}}, y_{cof} = \frac{\sum_{j=0}^{3} y_j \sum_{i=0}^{3} p_{ij}}{\sum_{j=0}^{3}\sum_{i=0}^{3} p_{ij}}$$

where p_{ij} is the pressure value at each sensel and x_i, y_j denote the x-coordinate of i^{th} column and y-coordinate of j^{th} row respectively on the 4x4 array.

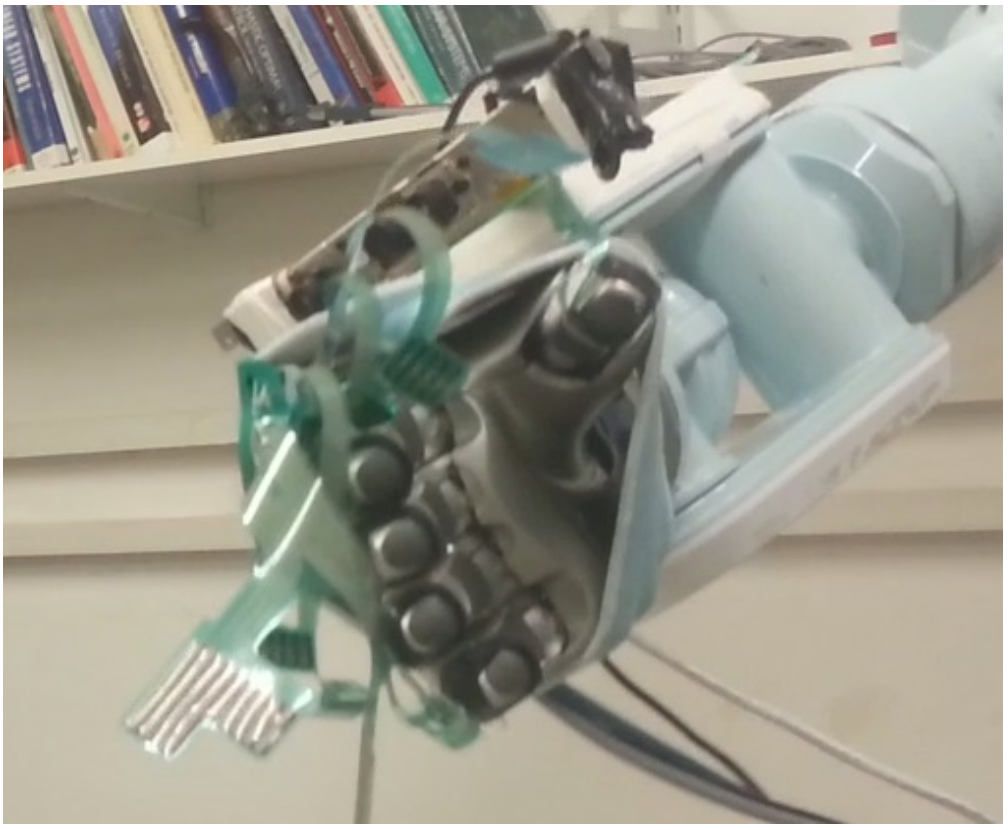

FIGURE 6.2: Experimental system setup, Front view

FIGURE 6.3: Experimental system setup, top view

The position of the contact centroids is defined by 2-d coordinates on the arrays of the tactile sensor. However, it is required to map the centroid local coordinates (x_{cof}, y_{cof}) into 3-D coordinates on the fingertip. Towards this goal, the point cloud of the DLR/HIT II fingertips was exploited. For each robotic finger, initially, the 4 corner sensels of the array were matched with their actual position $p_i^{corn}, i = 1, ..., 4$, on the point cloud and

the distance from them to all other nodes of the point cloud was computed. Assuming that the Grip sensor covers the surface of the fingertips due to its inherent thinness and flexibility, given a contact centroid on each array (x_{cof}, y_{cof}) its corresponding node P(X,Y,Z) on the point cloud was determined to minimize the function:

$$\min\{ \sum_{i=1}^{4}(dist_i(X,Y,Z) - arraydist_i(x_{cof}, y_{cof}))^2\} \tag{6.1}$$

where $dist_i(X,Y,Z)$ denotes the distance from p_i^{corn} to node P(X,Y,Z) on the point cloud and $arraydist_i(x_{cof}, y_{cof})$ denotes the distance between the i^{th} corner sensel and the contact centroid on the tactile array. In other words, it was assumed that the distance between two points remains invariant whether they are expressed by 3-d coordinates or 2-d coordinates on the arrays.

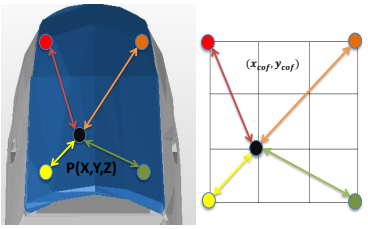

FIGURE 6.4: Distances on the fingertip and the tactile array respectively

With the aforementioned capabilities of the tactile suit, the steps of this approach towards the implementation of a successful grasp are presented:

1. Offline search for a robust configuration with respect to contact positioning inaccuracies as presented in the previous chapter
2. Implementation of the desired wrist position/orientation and joint angles
3. Joints' displacement freezing when their corresponding finger senses contact with the object through its tactile array
4. Reading the actual joint positions and contacts centroids from the encoders and tactile sensors output respectively
5. Mapping the contact centroids to their corresponding position on the mechanical fingertips using (6.1)
6. Computation of the contact points position on the object through forward kinematics
7. Determination of sufficient forces to grasp the object

It should be noticed that the measuring errors of the joint angle sensors are considered to be negligible. Hence, any errors in the contact points computation in Step 6, may appear only owing to uncertainties in the centroids' measurements.

6.2 Force optimization algorithm

In the sequel, the analysis towards defining adequate contact forces online is presented. The expressions that relate the contact forces f_c with the external disturbance w_{ext} and the joint torques τ are:

$$Gf_c = -w_{ext} \tag{6.2}$$

$$J^T f_c = \tau \tag{6.3}$$

where G and J denote the grasp matrix and hand jacobian respectively ($J = diag(J_i), i = 1, ..., n_p$) [22]. In case the vector f_c is expressed in global coordinates, the grasp matrix is defined as:

$$G = \begin{pmatrix} G_1 & G_2 & G_3 & \cdots & G_{n_p} \end{pmatrix}, \; G_i = \begin{bmatrix} I_{3x3} \\ S(cm - p_i) \end{bmatrix} \tag{6.4}$$

where cm is the center of mass position, I_{3x3} is the identity matrix and S is the cross product matrix. Furthermore, from (6.2) the contact forces can be written as:

$$f_c = -G^+ w_{ext} + E\lambda, \tag{6.5}$$

where G^+ is the pseudoinverse of G, E is a matrix whose columns form a basis for the nullspace of G and λ is an arbitrary vector. The first term of (6.5) is related to the compensation of external wrench w_{ext}, while the term $E\lambda$ denotes those forces whose resultant wrench to the object is zero [22]. The set of these forces is called internal forces. Internal forces play a fundamental role in grasping and are associated with the ability of the robotic hand to squeeze arbitrarily tight in order to grasp properly. Moreover, by exerting internal forces on the object appropriately, the generated contact forces comply with the friction constraints. Thus, the goal in this section is to calculate and apply appropriate internal forces to the object so that the friction law and torque constraints are not violated during a stable grasping.

Assume that the maximum absolute value of the uncertainty on the fingertips is δp_{max}. In this approach the magnitude of the uncertainty on the object geometry will also be considered as δp_{max}. To proceed, the authors in [35] proposed that even if contact uncertainties occur, equation (6.2) needs to be satisfied in order to grasp the object

successfully. Thus, by representing as δx the deviation of x due to δp and neglecting higher order terms, equation (6.2) becomes:

$$-w_{ext} = Gf_c = (\delta G + G)(\delta f_c + f_c)$$

$$\delta f_c = -G^{+}\delta G f_c \tag{6.6}$$

After straightforward matrix norm calculations, (6.4), (6.6) lead in:

$$\|\delta f_{c_i}\| \leq \|\Xi_i G^{+} \begin{bmatrix} 0 \\ I_{3x3} \end{bmatrix} \|\delta p_{max} \sum_{i=1}^{n_p} f_{c_i} \tag{6.7}$$

where Ξ_i represents a separation matrix ($f_{c_i} = \Xi_i f_c$). In addition, utilizing the orthonormality of the rotation matrices, equation (5.1) gives: $\|f_{c_i}\| \leq \sqrt{1+\mu^2} f_{n_i}$, where $f_{n_i} = n_i f_{c_i}$ is the normal force component and n_i is the contact normal vector. Thus, from (6.7) one obtains:

$$\|\delta f_{c_i}\| \leq \|\delta f_{c_{i_{max}}}\| = \|\Xi_i G^{+} \begin{bmatrix} 0 \\ I_{3x3} \end{bmatrix} \|\delta p_{max} \sqrt{1+\mu^2} \textstyle\sum_{i=1}^{n_p} f_{n_i} \tag{6.8}$$

Similarly, from equation (7.10) one gets for the k^{th} joint:

$$\delta\tau_{i_k} = \delta J_{i_k}^T f_{c_i} + J_{i_k}^T \delta f_{c_i} \tag{6.9}$$

Denoting by J_{i_k} the k^{th} row of J_i, for hard point contacts, one obtains [22]:

$$J_{i_k} = [z_{i_k} \times (p_{f_i} - d_{i_k})], \delta J_{i_k} = \frac{\partial J_{i_k}}{\partial p_{f_i}} \delta p_{f_i} + \frac{\partial J_{i_k}}{\partial q_{i_k}} \delta q_{i_k}$$

where p_{f_i} is the end effector position of each finger, z_{i_k}, d_{i_k} are the rotation axis and position of k^{th} joint respectively and q_{i_k} the k^{th} joint displacement. In our case, as explained in Subsection A, joint displacement errors are negligible, hence $(\partial J_{i_k}/\partial q_{i_k})\delta q_{i_k} = 0$. Consequently:

$$\delta J_{i_k} = [z_{i_k} \times \delta p_{fi}] \rightarrow \|\delta J_{i_k}\| \leq \|\delta J_{i_{k_{max}}}\| = \delta p_{max}$$

$$|\delta\tau_{i_k}| \leq |\delta\tau_{i_{k\,max}}| = \sqrt{1+\mu^2}\delta p_{max} f_{n_i} + \|J_{i_k}\|^T \|\delta f_{c_{i_{max}}}\| \tag{6.10}$$

It should be noted that contact uncertainty affects the friction cone as well. In light of this, a new friction coefficient for curved objects can be determined as [35]:

$$\theta_{max} = 2sin^{-1}\frac{\delta p_{max}}{2r}, \quad r : curvature\ radius$$
$$\mu' = tan(tan^{-1}\mu - \theta_{max})$$

In order to take into consideration the contact forces and joint torques deviation, the authors in [] proposed to increase the normal force component in the friction law by $\|\delta f_{c_{max}}\|$ (6.7) and reduce the maximum actuator torque by $|\delta\tau_{i_{k\,max}}|$ (6.10). Moreover, the friction cone defined in (5.1) may be approximated by an L-sided convex polyhedral cone in order to reduce the computational complexity of the problem [32]. Hence, (5.1) can be expressed as: $-V_i f_{c_i} \leq \mathbf{0}, \quad f_{n_i} \geq 0$.

Considering as decision variables the vector λ of the internal forces defined in (6.5), the linear optimization problem towards determining sufficient internal forces is formulated as following:

$$\min \sum f_{n_i}$$

s.t.

$$\begin{gathered} -V_i'(f_{c_i} - n_i\|f_{c_{i_{max}}}\|) \leq \mathbf{0} \\ |\tau_{i_k}| \leq |\tau_{i_{k_{max}}}| - |\delta\tau_{i_{k_{max}}}| \\ f_{n_i} \geq 0 \end{gathered}$$

$i = 1, ..., n_p, k = 1, ..., K$, where in V' the friction coefficient μ' is used instead of μ. The algorithm presented above searches for internal forces that minimize the sum of the normal forces and therefore the grasp effort, while simultaneously constraining the generated contact forces to satisfy the friction and torque constraints. The contact forces and joint torques produced by the internal forces are computed in the optimization scheme through equations (6.3), (6.5). In this work w_{ext} is considered to be the weight of the object. However, estimating the location of the center of mass with great precision is an extremely difficult task. Hence uncertainties in the center of mass position must be taken into consideration as well. These deviations can be represented as a set of external disturbances with respect to the nominal object coordinate frame. Consequently, instead of compensating the object's weight w_{ext}, we search for internal forces that compensate a set w_l, $l = 1, ..., L$, of external disturbances. In other words, the derived internal forces should produce for each external wrench w_l, contact forces (6.5) that satisfy the friction and torque constraints.

Remark 6.1. In [35] the authors had to deal not only with joint angle deviations but also with contact uncertainties both on the fingers and the object. In contrary, the utilization of tactile sensors allows us to neglect joint angle errors and take into account only potential errors on the fingertips. Furthermore, as stated in [35], given a configuration and uncertainty magnitude, it is possible that the constraints of the optimization problem cannot be satisfied. In other words, the particular configuration will not be

able to support the defined uncertainty. On the other hand, in our analysis, the posture of the robotic hand is determined by maximizing the force transmission ratio, as presented previously, whereas by exploiting tactile sensing we further reduce the range of uncertainty regarding the grasping parameters, thus relaxing significantly the on-line derivation of the internal forces. Apparently, the two parts of the proposed grasping strategy (i.e., the off-line and the on-line) are tightly connected and are cooperating towards generating successful grasps.

6.3 Verification through an experiment

DLR/HIT II is a fifteen DoF anthropomorphic robotic hand [36]. It has five identical fingers with 3 DoF per finger: two for flexion-extension and one for abduction-adduction. The last two joints are mechanically coupled using a steel wire with transmission ratio 1:1.

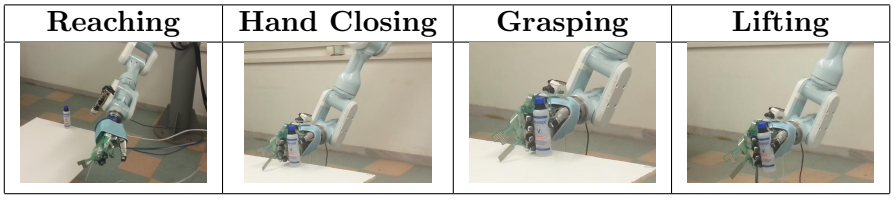

FIGURE 6.5: Experimental procedure

Regarding the grasping procedure, the DLR hand is attached at the end effector of the Mitsubishi PA10 manipulator and the tactile arrays are mounted on the robotic fingertips. The desired wrist position/orientation generated in the previous chapter, is used in order to derive anthropomorphic trajectories for the Mitsubishi PA10 robotic manipulator using "functional anthropomorphism" as described in [37]. Following this methodology it is possible to reach and grasp in a humanlike manner the desired object. Regarding the communications, a grasp planner PC (Ubuntu OS) establishes tcp connections with a PC (Windows OS) that collects the forces from the tekscan system and the Mitsubishi PA10 control unit (real-time linux), in order to detect contact with the object and provide the appropriate trajectories respectively. The experiment is performed using the cylindrical object presented in the simulation examples in the previous chapter of weight 100 gr.

In the previous section an optimization algorithm was presented that yields the required internal forces. In order to exert the desired forces the dynamic model of the robotic hand was utilized. Due to its inherent joint flexibility, the flexible joint model is used

Thumb	q_{des}	q_{act}	τ_{des}	τ_{act}
abd/ad	-12.9	-12.7	0.116	0.090
flex/ext 1	10.8	11.4	0.251	0.311
flex/ext 2	14.6	13.7	0.122	0.120
Index	q_{des}	q_{act}	τ_{des}	τ_{act}
abd/ad	-12.2	-11.0	-0.038	-0.012
flex/ext 1	10.6	11.3	0.109	0.108
flex/ext 2	18.9	18.7	0.053	0.064
Middle	q_{des}	q_{act}	τ_{des}	τ_{act}
abd/ad	-4.3	-4.9	-0.016	-0.018
flex/ext 1	16.8	16.1	0.093	0.097
flex/ext 2	23.1	22.1	0.052	0.064
Ring	q_{des}	q_{act}	τ_{des}	τ_{act}
abd/ad	6.0	4.7	0.006	0.007
flex/ext 1	19.4	19.9	0.039	0.037
flex/ext 2	21.1	20.1	0.021	0.034
Pinky	q_{des}	q_{act}	τ_{des}	τ_{act}
abd/ad	7.6	6.4	0.008	0.009
flex/ext 1	19.7	21.1	0.031	0.037
flex/ext 2	14.0	12.7	0.013	0.020

FIGURE 6.6: Experimental data (q :degrees, $\tau : Nm$)

[38]. In the presented analysis, one may arrive at:

$$\tau = g(q) - \tau_{ext} = K(\theta - q)$$

where q denotes the link side position vector, θ denotes the motor position vector expressed in link coordinates and $g(q)$ represents the the gravity term. Furthermore, K is the stiffness matrix and τ_{ext} denotes the external torque vector respectively. Since this analysis deals with rigid objects, for a given q vector (after contact detection), one may calculate the necessary motor displacements $\theta = \frac{g(q) - J_i^T f_{ext_d}}{K} + q$, in order to exert the desired internal forces f_{ext_d} on the object. The term $g(q)$ may be computed using the DH parameters and the nominal masses of the DLR/HIT II [38]. Below experimental data of the grasp implementation are presented.

Chapter 7

Dealing with task specificity

Every day life experience and recent neuroscientific studies on human grasping behaviour indicate that, when humans grasp objects, they intuitively adapt their hand posture according to the object and the task to be executed. Particularly, in [39] grasp selection by humans was studied and post processing of the hand's kinematics verified that humans adopt postures that generally maximize the force/velocity transmission ratios along the directions required for the task to be executed.

The problem of deriving optimal grasps under a detailed task description has been tackled in the past and various methodologies have been proposed. In [40] the authors searched for optimal grasps using the branch-and-bound method based on a required external set. Teichmann [41] minimized the number of contact points, needed to balance any external force and moment contained in a given set. Other works utilize the index proposed by Chiu that measures the compatibility of a manipulator to perform a given task [30], as well as the concept of the task ellipsoid proposed by Li and Sastry [42]. A task specific grasp selection scheme has been proposed in [43] for underactuated robotic hands as well. Unfortunately, most of the aforementioned approaches suffer from major drawbacks, such as the difficulty in modelling the task ellipsoid, as well as the fact that force closure is not generally guaranteed by the yielded configuration, limiting thus their applicability. As explained in the sequel, it is of great importance in this work not only to balance the task disturbances but also to derive a force closure grasp[1].

Given the presented analysis so far, a complete methodology for deriving task-specific force closure grasps for robotic hands under a wide range of uncertainties is proposed. Given a finite set of external disturbances representing the task to be executed, the concept of Q distance is introduced in a novel way to determine an efficient grasp with a task compatible hand posture (i.e., configuration and contact points). This approach

[1] Force closure ensures object immobility in the presence of any external disturbance [22].

takes, also, into consideration the mechanical and geometric limitations imposed by the robotic hand design and the object to be grasped. In addition, incorporating the main idea of the previous chapter, the ability of the robot hand to exert the required contact forces is maximized and robustness against positioning inaccuracies and object uncertainties is established. Finally, the efficiency of this approach is verified through an experimental study on a 15 DoF DLR/HIT II robotic hand attached at the end effector of a 7 DoF Mitsubishi PA10 robotic manipulator.

7.1 Grasping algorithm

We consider an n_p-fingered robotic hand with n_q rotational joints in total, grasping a rigid object with n_p point-to-point frictional contacts. The hard finger contact model is also adopted, which implies that all force components are transmitted through the contacts. Additionally, according to the friction coulomb model, each of the n_p forces must lie inside its correspoding friction cone in order to avoid slippage. Thus, denoting by μ the friction coefficient, by f_n the normal force component and by f_o, f_t the tangential components, the friction constraints are formulated as:

$$\sqrt{f_{i_o}^2 + f_{i_t}^2} \leq \mu f_{i_n}, \quad i = 1, ..., n_p. \tag{7.1}$$

Hence, linearizing the friction cone by an n_g-sided polyhedral cone, each grasping force can be represented as:

$$f_i = \sum_{j=1}^{n_g} a_{ij} s_{ij}, \quad a_{ij} \geq 0,$$

with s_{ij} denoting the j^{th} edge vector of the linearized friction cone. Consequently, the wrench produced by f_i is given by:

$$w_i = \begin{pmatrix} f_i \\ f_i \times p_i \end{pmatrix} = \sum_{j=1}^{n_g} a_{ij} \begin{pmatrix} s_{ij} \\ s_{ij} \times p_i \end{pmatrix}$$

where the vectors $w_{ij} = \begin{pmatrix} s_{ij} \\ s_{ij} \times p_i \end{pmatrix} \in \Re^6$ define the primitive wrenches (i.e., the wrench generated by a force along the j^{th} edge of the linearized friction cone) with p_i denoting the position of i^{th} contact point with respect to the object coordinate frame. Finally, the magnitude of the forces along the n_g edges of the friction cone is considered to be F_G.

In this way, the grasp is force closured if and only if the primitive wrenches positively span the entire wrench space, or equivalently the origin of the wrench space lies strictly inside the convex hull of the primitive wrenches (i.e., $\mathbf{0} \in \text{int}(\mathbf{co}(w_{11}, w_{12}, ..., w_{n_p n_g}))$) [44]. Notice, also, that the convex hull of the primitive wrenches, or else the *Grasp Wrench Space* (*GWS*) includes the set of wrenches that can be exerted on the object when the sum of the forces' magnitudes is bounded by F_G.

7.1.1 Task specific grasping posture

The proposed task specific grasp selection algorithm is based on the concept of the Q distance, originally proposed in [23], for curved objects. Given a compact convex set $Q \subset \mathbb{R}^m$ that contains the origin (i.e., $\mathbf{0} \in \text{int}(Q)$) and any point $\mathbf{a} \in \mathbb{R}^m$, the gauge function of Q is defined as:

$$g_Q(\mathbf{a}) = \left\{ \inf \gamma \mid \mathbf{a} \in \gamma Q \right\}$$

Notice further that $g_Q(\cdot)$ may be considered as a pseudonorm [23]. In addition, the origin centered Q-sphere in terms of g_Q is defined as: $S_Q = \rho Q = \left\{ \mathbf{a} \in \mathbb{R}^m \mid g_Q(\mathbf{a}) \leq \rho \right\}$, where ρ denotes the radius[2].

The authors in [23] showed that if $Q \subset \mathbb{R}^m$ is restricted to be a polyhedral set, the Q-distance d_Q from p to A, where $p \in \mathbb{R}^m$ is a point and $A \subset \mathbb{R}^m$ a convex polyhedron, is calculated in terms of g_Q as follows:

$-p \notin \text{int}(A)$:	$-p \in \text{int}(A)$:
$d_Q^+(p, A) = \min \sum_{k=1}^{K} \rho_k$ s.t. $\left\{ \begin{array}{c} \sum_{k=1}^{K} \rho_k q_k = \sum_{i=1}^{N} \alpha_i \mathrm{a}_i - p \\ \sum_{i=1}^{N} \alpha_i = 1 \\ \rho_k, \alpha_i \geq 0 \end{array} \right\}$	$d_Q^-(k) = \min(-\rho)$ s.t. $\left\{ \begin{array}{c} \rho q_k = \sum_{i=1}^{N} \alpha_i \mathrm{a}_i - p \\ \sum_{i=1}^{N} \alpha_i = 1 \\ \alpha_i, \rho \geq 0 \end{array} \right\}$ $d_Q^-(p, A) = \max_{k=1,...,K} d_Q^-(k)$

where q_k, $k = 1, ..., K$ and a_i, $i = 1, ..., N$ are the vertices of Q and A respectively. Notice that the aforementioned linear programs can be easily solved using the simplex method.

Assume that W contains the primitive wrenches of the grasp configuration ($m = 6$). As noted in [23], the equality $d_Q^+(\mathbf{0}, \mathbf{co}(W)) = 0$ represents a necessary condition for the force closure property, while the inequality $d_Q^-(\mathbf{0}, \mathbf{co}(W)) < 0$ is equivalent to $\mathbf{0} \in$

[2] In case Q is the L_2 sphere then g_Q is the same as the L_2 norm.

int($\mathbf{co}(W)$) and can be interpreted as a sufficient condition. Furthermore, the quantity $|d_Q^-(\mathbf{0}, \mathbf{co}(W))|$ is consistent with the popular quality metric defined in [45], except that the euclidean distance is replaced by the Q-distance. Thus, an optimal force closure grasp can be obtained by minimizing:

$$d_Q(\mathbf{0}, \mathbf{co}(W)) = \begin{cases} d_Q^+(\mathbf{0}, \mathbf{co}(W)), & \mathbf{0} \notin \text{int } (\mathbf{co}(W)) \\ d_Q^-(\mathbf{0}, \mathbf{co}(W)), & \mathbf{0} \in \text{int } (\mathbf{co}(W)) \end{cases}$$

Notice, also, that $-d_Q^-(\mathbf{0}, \mathbf{co}(W))$ can be geometrically interpreted as the largest radius of the Q-sphere contained in $\mathbf{co}(W)$. Therefore, minimizing $d_Q^-(\mathbf{0}, \mathbf{co}(W))$ leads to a grasp configuration that maximizes the radius of the Q sphere inside the convex hull of the primitive wrenches. To proceed, notice that the utilized quality measure is tightly connected to the Q set; thus, the optimal configuration can be adjusted through appropriate modification of Q. To illustrate this point let us consider Fig. 7.1. In these images two hypothetical convex hulls are depicted, for two grasp configurations. The quality metric used in the first case is the L_2 norm, while in the second case the adopted Q-set differs significantly from the L_2 sphere. It is obvious that the convenient L_2 norm evaluates equally these two cases. In contrast, the Q-distance discriminates the two configurations according to the task specifications imposed by the Q-set.

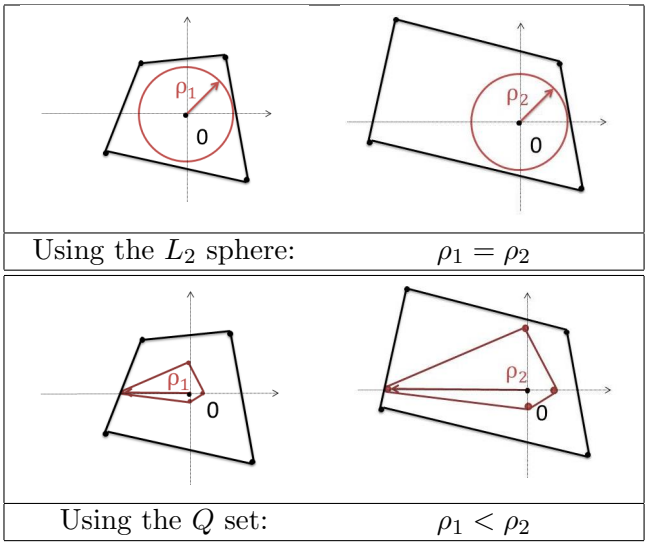

FIGURE 7.1: A hypothetical example illustrating the advantage of the Q distance over the L_2 norm in evaluating the task specificity of grasp configurations.

Considering the above and aiming at formulating a task oriented optimization problem, the Q set should contain the origin as well as those wrenches that need to be applied by the robotic hand in order to balance the task disturbances. Therefore, instead of

just guaranteeing the force closure property as in [23], the obtained configuration will be able to compensate disturbances in particular directions with relatively low forces. Finally, it should be mentioned that the sum of the task disturbances' magnitudes, F_t, should be lower or equal than the sum of contact forces ($F_t \leq F_G$) [27].

To calculate task specific grasping postures in the context of Q-distance, we formulate our optimization problem with the unified vector $v = \begin{bmatrix} q & w \end{bmatrix}^T$ as decision variable, where $q \in \mathbb{R}^{n_q}$ and $w \in \mathbb{R}^6$ denote the joint displacements and wrist position/orientation respectively. We further assume that the desired position/orientation of the robotic hand can be implemented by attaching it on a dexterous manipulator. Thus, the optimization problem is defined as follows:

$$\min \; d_Q(\mathbf{0}, \mathbf{co}(W))$$

s.t.

$$q_{min} \leq q \leq q_{max} \tag{7.2}$$

$$fkine(q) \in \partial O \tag{7.3}$$

$$q^j_{abd/add} \leq q^{j+1}_{abd/add} \tag{7.4}$$

$$p' \notin O \tag{7.5}$$

Equation (7.2) describes the joint mechanical limits whereas (7.3) ensures that the fingertips are in contact with the object surface. Furthermore, $q^j_{abd/add}, (j = 1, ..., n_p - 1)$ represents the abduction/adduction degree of freedom of all fingers opposed to the thumb (index, middle, ring, pinky). Hence, equation (7.4) prevents collision between consecutive robotic fingers. The last constraint is added in order to avoid penetration between the robotic hand and the object. In particular, p' denotes a set of finite discrete points lying on the robotic hand (the fingertips are excluded). Thus, given an analytical expression of the object boundary, equation (7.5) can be easily expressed as inequality constraints. Henceforth, we shall refer to these constraints using the abbreviation RHC, (*Robotic Hand Constraints*).

It was proven (see [23]) that in case the primitive wrenches can be expressed as smooth functions, the derivatives of d_Q^+ and d_Q^- exist and can be computed accurately almost everywhere. In such case, we are able, through the computation of the manipulator's forward kinematics, to calculate the derivative of the objective function with respect to the decision variables vector v. Thus, computing also the derivatives of the constraints with respect to v, the problem can be solved using a non linear programming algorithm and an optimal force closure grasp configuration can be obtained.

7.1.2 Dealing with force transmission maximization and positioning inaccuracies

So far we have taken into account the task specifications and kinematic constraints that need to be satisfied during the grasping posture selection. However, robotic hands are also subjected to joint torque constraints. Thus, it is important to adopt a robot hand configuration that is capable of exerting the required grasping forces on the object with relatively low joint torque effort. Towards this goal, we exploited the force transmission ratio r_k and compatibility index c which was originally defined in [30] as:

$$r_k = [u_k^T (J_i J_i^T) u_k]^{-1/2}$$
$$c_i = \sum_{k=1}^{l} r_k^2 = \sum_{k=1}^{l} [u_k^T (J_i J_i^T)_k^u]^{-1}$$

where u_k, $k = 1, ..., l$, denotes the direction of interest for the contact forces and J_i denotes the jacobian of the i^{th} finger, $i = 1, ..., n_p$. Since we have assumed frictional hard contacts, each force is restricted to lie inside its corresponding friction cone. Hence, for each contact point we choose the unit vectors u_k to be aligned with the edges of the linearized friction cone as in [31]. In this way, the compatibility index for the robotic hand is given by:

$$c = \sum_{i=1}^{n_p} w_{f_i} c_i = \sum_{i=1}^{n_p} w_{f_i} \sum_{k=1}^{n_g} [u_k^T (J_i J_i^T) u_k]^{-1}$$

where w_{f_i} are weighting factors, each one for every finger. Thus, maximization of the compatibility index c yields an optimal posture with respect to the force transmission metric. However, since deviation between the actual and desired joint positions is inevitable, we must guarantee that the robotic hand can perform the given task despite fingertip positioning inaccuracies. Therefore, we utilized the concept of independent contact regions (ICR), adopting, in particular, the approach described in [27] to determine whether a point on the object boundary qualifies to be a member of an ICR.

In summary, consider a given force closure grasp configuration that contains the set of task wrenches (*Task Wrench Space*, TWS). Each ICR_i consists of a set of discrete points, such that if the fingertips are placed inside the corresponding region, a force closure grasp is obtained that can balance the task disturbances. The procedure of computing the $ICRs$ based on the particular method is illustrated in Fig. 7.2 for a hypothetical 2-d wrench space. A convex hull of 3 contact points is illustrated that contains the TWS (red colour). Each contact point p_i is associated with two primitive wrenches w_{ij} and a number of facets F_k, involving at least one vertex w_{ij}. For instance,

w_{11} of contact point p_1 is associated with facets F_1 and F_2. H'_1, H'_2 are the hyperplanes built parallel to F_1, F_2 respectively and tangent to TWS, leaving $\mathbf{0}$ and their corresponding facet at different halfpsaces. Assuming that $\mathbf{co}(W) \subseteq H_k^-$, the intersection of the halfspaces $H_1'^+, H_2'^+$ is named S_{11} ($S_{11} = \bigcap H_k'^+, k = 1, 2$). S_{12} may be created for w_{12} similarly. A neighbouring point is said to be included in the ICR_1 if its primitive wrenches lie inside S_{11} and S_{12} respectively.

In our work, the range of the joint displacement error of the robotic hand is known, hence the deviation of the contact points can be computed. Therefore, instead of checking which points on the object boundary qualify to be inside the $ICRs$, as in [25], [27], we check whether the necessary hyperplane displacements H'_k satisfy the task constraints (i.e., the TWS belongs in $\bigcap H_k'^-$). Thus, given: i) the nominal contact points p_i, ii) the hyperplanes' equations $H_k x = K_k$, iii) the deviated contact points $p_{is}, s = 1, ..., S$ for each p_i as well as iv) the set of task disturbances $t_\delta \in TWS, \delta = 1, ..., \Delta$, we can compute the distance of H'_k from $\mathbf{0}$ when it is built tangent to the TWS as $D_k = \max(H_k t_\delta) > 0$. This quantity denotes the minimum required distance between H'_k and $\mathbf{0}$ so that the TWS will be contained in the GWS . Consequently, whether the deviated contact points belong in their respective ICR, can be determined as follows:

for $i \leftarrow 1$ **to** n_p (*ie for each contact point*, p_i) **do**
  for $j \leftarrow 1$ **to** n_g (*ie for each prim wrench*, w_{ij}) **do**
    find hyperplanes H_k that involve w_{ij}
    for $k \leftarrow 1$ **to** K (*ie for each* H_k *of* w_{ij}) **do**
      for $s \leftarrow 1$ **to** S (*ie for each deviated* p_{is}) **do**
        compute the maximum possible distance κ_s=max$(H_k w_{i_{sj}})$ of H'_k from $\mathbf{0}$ so that at least one primitive wrench of p_{is} belongs in $H_k'^+$
      end
      compute the required signed distance $\Lambda_k = \min(\kappa_s)$ of H'_k from $\mathbf{0}$ so that at least one primitive wrench of all p_{is} belongs in $H_k'^+$
      if $\Lambda_k < D_k$ **then**
        $p_{is} \notin ICR_i$
        break
      end
    end
  end
  $p_{is} \in ICR_i, s = 1, ..., S$ (ie all uncertainties p_{is} of p_i belong in ICR_i)
end

where all the above distances are computed through vector dot products, rendering the procedure very computationally efficient. Notice that, if $\Lambda_k < D_k$ at least one hyperplane H'_k that involves a primitive wrench of the deviated contact points does not contain the TWS.

In this work, the TWS is represented by the Q set defined in Subsection II-A. Considering the analysis above and keeping as decision variables the unified vector $v = \begin{pmatrix} q & w \end{pmatrix}^T$,

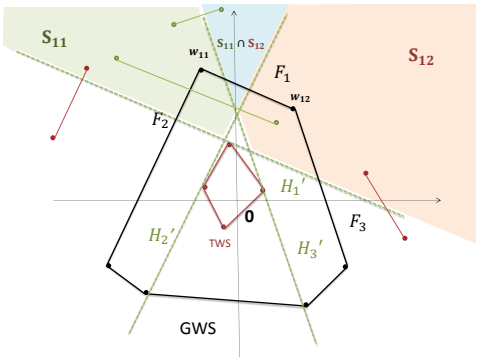

FIGURE 7.2: Computation of ICR_1. The green primitive wrenches belong in regions S_{11} and S_{12} respectively and are associated with contact points inside the ICR_1.

we formulate an optimization problem that yields a grasp configuration with optimal force transmission and robustness against positioning inaccuracies as follows:

$$\min \ \frac{1}{c}$$

s.t.

$$RHC$$

$$d_Q^-(\mathbf{0}, \mathbf{co}(W)) < 0 \tag{7.6}$$

$$p_{is} \in ICR_i \tag{7.7}$$

As it was mentioned earlier, the inequality $d_Q^-(\mathbf{0}, \mathbf{co}(W)) < 0$ represents a necessary and sufficient condition for the force closure property. Hence, equation (7.6) enforces the algorithm to search only force closured grasps. Moreover, equation (7.7) enforces the deviated contact points p_{is} to belong in their corresponding independent contact region. Finally, the initial posture provided to the algorithm is the one calculated in Subsection II-A. As the authors in [25] state, an optimal configuration with respect to the utilized quality metric (defined in [45]) results in larger ICRs. In light of this, the task oriented optimal grasp configuration generated in the previous subsection is ideal to initiate our second search algorithm.

Remark 7.1. The quantity d_Q^- which is utilized as a task oriented quality metric, depends exclusively on the position of the contact points on the surface of the object and is associated with the transformation of contact forces to object wrenches. On the other hand, the compatibility index c is used so that the resulted configuration of the robotic

hand can effectively transform joint torques to contact forces. Considering the above, the proposed strategy exploits both quality metrics such that the desired task can be implemented without a great amount of effort.

7.2 Determining contact forces via tactile sensing

Apart from choosing a suitable configuration, it is essential to be able to apply appropriate forces in order to ensure object immobility. Due to the hyperstatic nature of the force-determination problem, force optimization algorithms have received great attention. Balancing the external disturbances with relatively small applied forces may prevent the object from deforming while requesting low joint torque effort. Nevertheless, certain uncertainties during the grasping procedure need to be taken into consideration, such that the robotic hand can lift the object successfully. Towards relaxing the magnitude of uncertainty, we utilized valuable information from tactile sensors deployed appropriately on the robotic fingertips.

7.2.1 Introducing tactile sensing

Humans are able to use sensory data from their skin in order to interact successfully with the environment. In a similar manner, appropriate tactile devices may contribute to the implementation of dexterous grasping and manipulation tasks, by providing useful information about geometrical and physical quantities of the objects. In our work, we used the off-the-shelf 4256e Grip sensor designed by Tekscan. This ultra thin (0.15 mm) tactile sensor consists of 320 sensing elements (sensels) and is able to measure the pressure magnitude of each sensel based on piezo-resistive technology. The active region of each fingertip is a 4x4 array and the sensels' output allows us to compute the center of force, or equivalently, the contact centroid as:

$$x_{cof} = \frac{\sum_{i=0}^{3} x_i \sum_{j=0}^{3} p_{ij}}{\sum_{i=0}^{3}\sum_{j=0}^{3} p_{ij}}, y_{cof} = \frac{\sum_{j=0}^{3} y_j \sum_{i=0}^{3} p_{ij}}{\sum_{j=0}^{3}\sum_{i=0}^{3} p_{ij}}$$

where p_{ij} is the pressure value at each sensel and x_i, y_j denote the x-coordinate of i^{th} column and the y-coordinate of j^{th} row respectively on the 4x4 array.

The position of the contact centroids is defined by 2-D coordinates on the arrays of the tactile sensor. However, it is required to map the centroid local coordinates (x_{cof}, y_{cof}) into 3-D coordinates on the fingertip. Towards this goal, we exploited the point cloud of

the robotic fingertips (in our case for the DLR/HIT II robotic hand). For each robotic finger, we, initially, matched the 4 corner sensels of the array with their actual position $p_i^{corn}, i = 1, ..., 4$, on the point cloud and computed the distance from them to all other nodes of the point cloud. Assuming that the Grip sensor covers firmly the surface of the fingertips owing to its inherent thinness and flexibility, given a contact centroid on each array (x_{cof}, y_{cof}) we determined its corresponding node P(X,Y,Z) on the point cloud of the robotic fingertip by minimizing the function:

$$\min\{ \sum_{i=1}^{4}(dist_i(X,Y,Z) - arraydist_i(x_{cof}, y_{cof}))^2\} \tag{7.8}$$

where $dist_i(X,Y,Z)$ denotes the distance from p_i^{corn} to node P(X,Y,Z) on the point cloud and $arraydist_i(x_{cof}, y_{cof})$ denotes the distance between the i^{th} corner sensel and the contact centroid on the tactile array. In other words, we assumed that the distance between two points remains invariant whether they are expressed by 3-d coordinates or 2-d coordinates on the arrays.

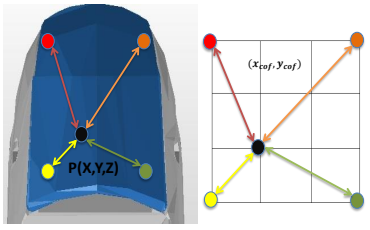

FIGURE 7.3: Distances on the fingertip and the tactile array respectively

7.2.2 The grasping strategy

With the aforementioned tactile sensing capabilities, we present the following grasping strategy:

1. Offline search for a task specific robust configuration (i.e., joint angles and wrist position/orientation) as presented in the previous subsection.
2. Implementation of the desired configuration.
3. Stop robotic finger motion when contact with the object has been detected by the corresponding tactile sensor.
4. Obtain the actual joint positions and contact centroids from the encoders and the tactile sensors respectively.
5. Map the contact centroids to their corresponding position on the mechanical fingertips using (7.8)

6. Compute the position of the contact points on the object through forward kinematics.

7. Determine sufficient forces to grasp the object.

It should be noticed that the measuring errors of the joint angle sensors are considered to be negligible. Hence, any errors in the contact points computation in Step 6, may appear only owing to uncertainties in the centroids' measurements.

In the sequel, we present the algorithm that calculates online adequate contact forces to ensure object immobility. The expressions that relate the contact forces f_c with the external disturbance w_{ext} and the joint torques τ are:

$$Gf_c = -w_{ext} \tag{7.9}$$

$$J^T f_c = \tau \tag{7.10}$$

where G and J denote the grasp matrix and hand jacobian respectively ($J = diag(J_i), i = 1, ..., n_p$) [22]. In case the vector f_c is expressed in global coordinates, the grasp matrix is defined as:

$$G = \begin{pmatrix} G_1 & G_2 & G_3 & \cdots & G_{n_p} \end{pmatrix}, \; G_i = \begin{bmatrix} I_{3x3} \\ S(cm - p_i) \end{bmatrix} \tag{7.11}$$

where cm is the center of mass position, I_{3x3} is the identity matrix and S is the cross product matrix. Furthermore, from (7.9) the contact forces can be written as:

$$f_c = -G^+ w_{ext} + E\lambda, \tag{7.12}$$

where G^+ is the pseudoinverse of G, E is a matrix whose columns form a basis for the nullspace of G and λ is an arbitrary vector. The first term of (7.12) is related to the compensation of external wrench w_{ext}, while the term $E\lambda$ denotes those forces whose resultant wrench to the object is null [22]. The set of these forces is known as internal forces. Internal forces play a fundamental role in grasping and are associated with the ability of the robotic hand to squeeze arbitrarily tight in order to grasp properly. Moreover, by exerting internal forces on the object appropriately, the generated contact forces comply with the friction constraints. Thus, our goal in this section is to calculate and apply appropriate internal forces to the object so that the friction law and torque constraints are not violated during a stable grasping.

Assume that the maximum absolute value of the uncertainty on the fingertips is δp_{max}. In our approach the magnitude of the uncertainty on the object geometry will also be

considered as δp_{max}. To proceed, the authors in [35] proposed that even if contact uncertainties occur, equation (7.9) needs to be satisfied in order to grasp the object successfully. Thus, by representing as δx the deviation of x due to δp and neglecting higher order terms, equation (7.9) becomes:

$$-w_{ext} = Gf_c = (\delta G + G)(\delta f_c + f_c)$$

$$\Rightarrow \delta f_c = -G^{+}\delta G f_c \tag{7.13}$$

After straightforward matrix norm calculations, (7.11), (7.13) lead in:

$$\|\delta f_{c_i}\| \leq \|\Xi_i G^{+} \begin{bmatrix} 0 \\ I_{3x3} \end{bmatrix} \|\delta p_{max} \sum_{i=1}^{n_p} f_{c_i} \tag{7.14}$$

where Ξ_i represents a separation matrix ($f_{c_i} = \Xi_i f_c$). In addition, utilizing the orthonormality of the rotation matrices, equation (7.1) gives: $\|f_{c_i}\| \leq \sqrt{1+\mu^2} f_{n_i}$, where $f_{n_i} = n_i f_{c_i}$ is the normal force component and n_i is the contact normal vector. Thus, from (7.14) we obtain:

$$\|\delta f_{c_i}\| \leq \|\delta f_{c_{i_{max}}}\| = \|\Xi_i G^{+} \begin{bmatrix} 0 \\ I_{3x3} \end{bmatrix} \|\delta p_{max} \sqrt{1+\mu^2} \textstyle\sum_{i=1}^{n_p} f_{n_i} \tag{7.15}$$

Similarly, from equation (7.10) we get for the k^{th} joint:

$$\delta\tau_{i_k} = \delta J_{i_k}^T f_{c_i} + J_{i_k}^T \delta f_{c_i} \tag{7.16}$$

Denoting by J_{i_k} the k^{th} row of J_i, for hard point contacts, we obtain [22]:

$$J_{i_k} = [z_{i_k} \times (p_{f_i} - d_{i_k})], \delta J_{i_k} = \frac{\partial J_{i_k}}{\partial p_{f_i}} \delta p_{f_i} + \frac{\partial J_{i_k}}{\partial q_{i_k}} \delta q_{i_k}$$

where p_{f_i} is the end effector position of each finger, z_{i_k}, d_{i_k} are the rotation axis and position of k^{th} joint respectively and q_{i_k} the k^{th} joint displacement. In our case, as explained in Subsection IIC 2), joint displacement errors are negligible, hence $(\partial J_{i_k}/\partial q_{i_k})\delta q_{i_k} = 0$. Consequently, we arrive at:

$$\delta J_{i_k} = [z_{i_k} \times \delta p_{fi}] \Rightarrow \|\delta J_{i_k}\| \leq \|\delta J_{i_{k_{max}}}\| = \delta p_{max}$$

$$|\delta\tau_{i_k}| \leq |\delta\tau_{i_{k_{max}}}| = \sqrt{1+\mu^2}\delta p_{max} f_{n_i} + \|J_{i_k}\|^T \|\delta f_{c_{i_{max}}}\| \tag{7.17}$$

It should be noted that contact uncertainty affects the friction cone as well. In light of this, a new friction coefficient for curved objects can be determined as [35]:

$$\theta_{max} = 2sin^{-1}\frac{\delta p_{max}}{2r}, \quad r : curvature\ radius$$
$$\mu' = tan(tan^{-1}\mu - \theta_{max})$$

In order to take into consideration the contact forces and joint torques deviation, the authors in [35] proposed to increase the normal force component in the friction law by $\|\delta f_{c_{max}}\|$ (7.14) and reduce the maximum actuator torque by $|\delta\tau_{i_{k\,max}}|$ (7.17). Moreover, the friction cone defined in (7.1) may be approximated by an L-sided convex polyhedral cone in order to reduce the computational complexity of the problem [32]. Hence, (7.1) can be expressed as: $-V_i f_{c_i} \leq \mathbf{0}, \quad f_{n_i} \geq 0$.

Considering as decision variables the vector λ of the internal forces defined in (7.12), the linear optimization problem towards determining sufficient internal forces is formulated as follows:

$$\min \sum f_{n_i}$$

s.t.

$$-V_i'(f_{c_i} - n_i\|f_{c_{i_{max}}}\|) \leq \mathbf{0}$$
$$|\tau_{i_k}| \leq |\tau_{i_{k_{max}}}| - |\delta\tau_{i_{k_{max}}}|$$
$$f_{n_i} \geq 0$$

$i = 1, ..., n_p, k = 1, ..., K$, where in V' the friction coefficient μ' is used instead of μ. The algorithm presented above searches for internal forces that minimize the sum of the normal forces and therefore the grasp effort, while simultaneously constraining the generated contact forces to satisfy the friction and torque constraints. The contact forces and joint torques produced by the internal forces are computed in the optimization scheme through equations (7.10), (7.12).

Remark 7.2. In [35] the authors had to deal not only with joint angle deviations but also with contact uncertainties both on the fingers and the object. In contrast, the tactile sensors allows us to neglect joint angle errors and take into account only potential errors on the fingertips. Furthermore, as stated in [35], given a configuration and uncertainty magnitude, it is possible that the constraints of the optimization problem cannot be satisfied (i.e., the particular configuration will not be able to support the defined uncertainty). On the other hand, in our analysis, the posture of the robotic hand is determined by maximizing the force transmission ratio, as presented in Subsection II-B, whereas by exploiting tactile sensing we further reduce the range of uncertainty regarding the grasping parameters, thus relaxing significantly the on-line calculation of the internal forces. Apparently, in this way the two parts of the proposed grasping

strategy (i.e., the off-line and the on-line) are tightly interconnected towards generating successful grasps.

7.3 Experimental results and verification

In this section, we initially present the considered task specifications and then verify the grasping algorithm developed in Section II via an experimental study with the DLR/HIT II robotic hand.

7.3.1 Task description

Our experimental procedure considers the stable grasp of a cylindrical object filled with liquid, while it is being rotated about one axis. Four different states of the object are depicted in Fig. 7.4, all of which are used to model our task disturbances. More specifically, the rotation is implemented about the z axis, while it is assumed that the liquid is distributed symetrically about the particular axis. In these images the black dot denotes the center of mass for each state of the object, while the object coordinate frame is determined by the red axis. Thus, it can be inferred that the object's weight at the depicted states causes external forces along the x and y axis, as well as external moments about the z axis of the object coordinate frame.

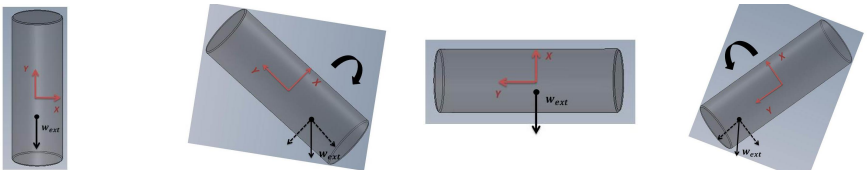

(a) Phase I (b) Phase II (c) Phase III (d) Phase IV

FIGURE 7.4: Task description

7.3.2 Output of the algorithms

The object to be grasped was considered to be a 2.25 cm-radius, 13 cm-high cylinder. Given the task and object characteristics, the algorithms in Subsections II-A, II-B yielded off-line an optimal posture illustrated in Fig. 7.5. For the derived configuration we considered an 8-sided linearized friction cone and, due to the robust nature of our analysis, we selected a conservative friction coefficient [26] ($\mu = 0.3$). Furthermore based on the joint displacement error of the DLR/HIT II robotic hand, the maximum contact point deviation on the object was found to be 4 mm. Hence, for the computation of

the $ICRs$ presented in Subsection II-B, four deviated contact points (denoted as p_{is}) were considered at a distance of 4 mm from their corresponding nominal contact point. It should be mentioned that, the influence of uncertainties related to the friction coefficient and object model were considered for the $ICRs$ determination as presented in [28]. The solution of the optimization schemes was derived using the MATLAB Optimization Toolbox.

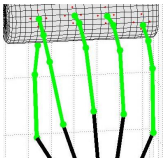

FIGURE 7.5: Optimal configuration (red dots denote the contact points uncertainties)

In order to perform the given task the required internal forces are computed by solving the algorithm presented in Subsection II-C. As it was stated there, the contact forces derived by the internal forces should satisfy the friction and torque constraints. In our work w_{ext} in (7.12) is considered to be the set of task disturbances that appear throughout the experimental procedure (see Fig. 7.4). However, estimating the location of the center of mass with great precision is an extremely difficult task. To overcome this difficulty, the particular uncertainties can be represented as a set of external wrenches with respect to the nominal position of the center of mass. Consequently, instead of compensating the nominal task disturbances $w_t, t = 1, ..., T$, we search for internal forces that compensate a set w_{tl}, $l = 1, ..., L$, of external disturbances, where w_{tl} denotes the l center of mass uncertainty for the t task disturbance. In other words, the derived internal forces should produce, for each external wrench w_{tl}, contact forces (7.12) that satisfy the friction and torque constraints. In this respect, note also that the Q set determined in Subsection II-A should not only include the nominal task loads, but also the external wrenches associated with the uncertainty in the center of mass.

In Fig. 7.6 we present the desired angles q and torques τ. The vector τ was obtained employing (7.10) and (7.12). Regarding the calculation of the internal forces, the uncertainty of the contact points δp_{max} and the center of mass is considered to be 1 and 3 cm respectively.

7.3.3 Experimental verification

DLR/HIT II is a fifteen DoF anthropomorphic robotic hand [36]. It has five identical fingers with 3 DoF per finger: two for flexion-extension and one for abduction-adduction. The last two joints are mechanically coupled using a steel wire with transmission ratio 1:1. The DLR/HIT II robotic hand is attached at the end effector of the Mitsubishi PA10

Thumb	q	τ	**Index**	q	τ
a/a	-12.4	0.12	a/a	-9.1	-0.07
f/e 1	8.9	0.34	f/e 1	22.8	0.13
f/e 2	10.9	0.17	f/e 2	13	0.07
Middle	q	τ	**Ring**	q	τ
a/a	-4.3	-0.01	a/a	0.3	0
f/e 1	12	0.07	f/e 1	10.8	0.09
f/e 2	35.2	0.04	f/ext 2	33.2	0.07

Pinky	q	τ
a/a	5.2	0
f/e 1	12.5	0.03
f/e 2	21	0.01

FIGURE 7.6: Experimental data (q :degrees, τ : Nm, "a/a": abduction/adduction DoF,"f/e": flexion/extension DoF)

manipulator and the tactile arrays are mounted on the robotic fingertips. Furthermore, a grasp planner PC (Ubuntu OS) establishes tcp connections with a PC (Windows OS) that collects the forces from the tekscan system and the Mitsubishi PA10 control unit (real-time linux), in order to detect contact with the object and provide the appropriate trajectories respectively. Note, also, that due to the high accuracy we have in terms of positioning the Mitsubishi PA10 end effector, we neglect errors in the actual wrist position/orientation.

In order to exert the desired forces we utilized the dynamic model of the robotic hand. Owing to its inherent joint flexibility, the flexible joint model is used [38]. In our case, we may arrive at:

$$\tau = g(q) - \tau_{ext} = K(\theta - q)$$

where q denotes the link side position vector, θ denotes the motor position vector expressed in link coordinates and $g(q)$ represents the gravity term. Furthermore, K is the stiffness matrix and τ_{ext} denotes the external torque vector. Since we deal with rigid objects, for a given q vector (after contact detection), we may calculate the necessary motor displacements $\theta = K^{-1}(g(q) - J_i^T f_{ext_d}) + q$, in order to exert the desired internal forces f_{ext_d} on the object. The term $g(q)$ may be computed using the DH parameters and the nominal masses of the DLR/HIT II [38]. Finally, three snapshots of the experiment we conducted are given in Fig. 7.7.

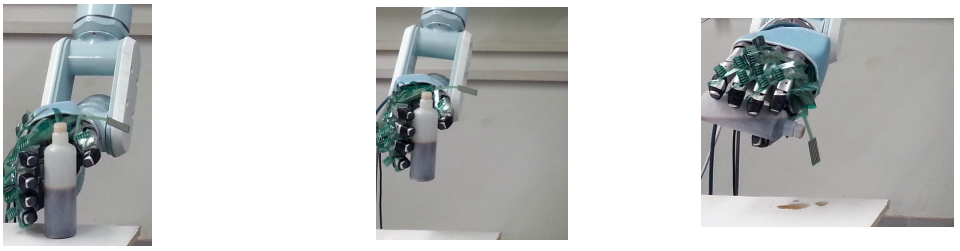

(a) Reaching. (b) Grasping/Lifting. (c) Performing the task.

FIGURE 7.7: Three snapshots of the reaching, grasping and task implementation phases

Chapter 8

Conclusion

In this thesis, the problem of robust grasping was tackled. The proposed work constituted an analytical approach to robust grasping and its applicability was verified through simulated examples and experimental paradigms for the case of the DLR HIT II robotic hand. Regarding the theoretical part, a wide range of uncertainties was considered so that grasp stability is maintained despite potential deviations of grasping parameters. The optimization schemes yielded an acceptable grasp posture and appropriate contact forces towards achieving a stable grasp. For the experimental part, useful information from a tactile sensor was utilized. This strategy eventually allowed to reduce the magnitude of uncertainty and relax the computation of forces. In addition, in the case that task specifications must be satisfied, the theoretical part, which is based on the concept of Q distance, can be modified to handle the task description.

Future directions are presented:

- The proposed methodology was applied to a cylindrical object. Instead of having a boundary that can be expressed by an analytical equation, objects with complex geometry could be used
- In this thesis the point contact model was used. One interesting direction could be applying a similar approach using a patch contact model
- Instead of exerting forces through joint displacements, a force control scheme could be utilized
- It would be interesting to utilize tactile information in order to discover certain object properties such as its boundary and stiffness

- The proposed grasping approach could be used to initialize a manipulation procedure

Appendix A

DH parameters for the DLR HIT II

DH Parameter

Joint	D[mm]	φ	a[mm]	α
0	0	0	0	0
1	0	0	0	$\pi/2$
2	0	0	55	0
3	0	$-\pi/2$	25	0
4	25	π	0	$-\pi/2$

Joint Limits

Joint	Lower Limit	Upper Limit
0	-15°	15°
1	5°	85°
2	5°	65°

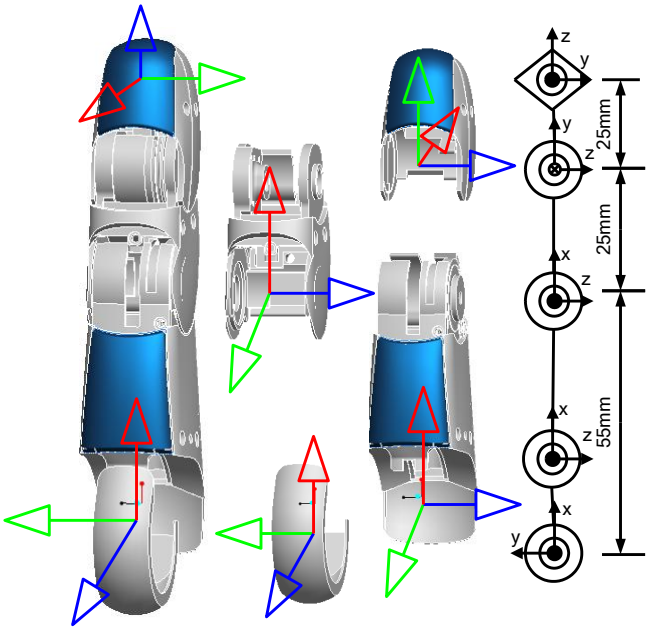

FIGURE A.1: DH (i)

Righthand

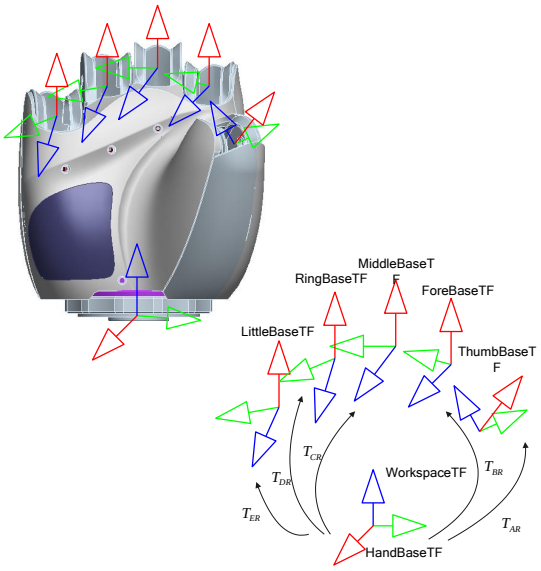

HandbaseTF

ThumbBaseTF:

$$T_{AR} = \begin{bmatrix} 0.429051 & -0.571047 & -0.699872 & 0.062569057 \\ 0.187173 & 0.814200 & -0.549586 & 0.044544548 \\ 0.883675 & 0.104803 & 0.456218 & 0.080044647 \\ 0 & 0 & 0 & 1 \end{bmatrix}$$

FIGURE A.2: DH (ii)

ForeBaseTF:

$$T_{BR} = \begin{bmatrix} 0 & -0.087156 & 0.996195 & -0.002529881 \\ 0 & -0.996195 & -0.087156 & 0.036800135 \\ 1 & 0 & 0 & 0.108743545 \\ 0 & 0 & 0 & 1 \end{bmatrix}$$

RingBaseTF:

$$T_{DR} = \begin{bmatrix} 0 & 0.087156 & 0.996195 & -0.002529881 \\ 0 & -0.996195 & 0.087156 & -0.016800135 \\ 1 & 0 & 0 & 0.114043545 \\ 0 & 0 & 0 & 1 \end{bmatrix}$$

MiddleBaseTF

$$T_{CR} = \begin{bmatrix} 0 & 0 & 1 & -0.0037 \\ 0 & -1 & 0 & 0.01 \\ 1 & 0 & 0 & 0.119043545 \\ 0 & 0 & 0 & 1 \end{bmatrix}$$

LittleBaseTF:

$$T_{ER} = \begin{bmatrix} 0 & 0.173648 & 0.984808 & 0.000971571 \\ 0 & -0.984808 & 0.173648 & -0.043396306 \\ 1 & 0 & 0 & 0.095043545 \\ 0 & 0 & 0 & 1 \end{bmatrix}$$

FIGURE A.3: DH (iii)

Appendix B

Routines

The matlab routines for the implementation of the proposed approach are presented.

`Qdistcylkin.m` (Script):

This main MATLAB routine is used to derive an optimal grasp configuration in terms of the Q metric. It initializes most variables (object and robotic hand parameters) and calls the functions below.

`Qdistcylkinobjf.m` (function):

Calclulates d_Q^+ for the determination of the objective function.

`Qmaxdistcylkinobjf.m` (function):

Calclulates d_Q^- for the determination of the objective function.

`Qdistcylkincon.m` (function):

Calclulates the kinematic constraints that constitute the constraints of the optimization problem.

`Qmaxdistcylkinobjf.m` (function):

Calclulates d_Q^- for the determination of the objective function.

`contact_frame.m` (function):

Calclulates the rotation matrix for each contact.

`convexcyl.m` (function):

Calclulates the vertices of the convex hull of the primitive wrenches.

`cylinderpoints.m` (function):

Calclulates the points of the cylinder based on its properties.

`kinematic.m` (function):

Calclulates the forward kinematics of the DLR HIT.

`plothandfingers.m` (function):

Plots the grasp configuration of the DLR HIT.

`metricsQcyl.m` (Script):

This main MATLAB routine is used to derive an optimal grasp configuration in terms of the Q metric and the force manipulability measure. It constraints the deviated contact points to belong in ICR_s. It initializes most variables (object and robotic hand parameters) and calls the functions below.

`metricsQcylobjf.m` (function):

Calculates the objective function.

`metricsQcylcon.m` (function):

Calculates the constraints of the particular optimization problem.

`forcemanipfrcyl.m` (function):

Calculates the force manipulability measure.

`hypermovement.m` (function):

Calculates the required hyperplanes displacements.

`vertlcon.m` (function):

Calculates the hyperplanes parameters.

`torques.m` (Script):

This main MATLAB routine is used to derive the optimal contact forces. It considers deviations of the parameters. It initializes most variables (object and robotic hand parameters) and calls the functions below.

`forcesobjf.m` (function):

Calculates the objective function of the optimization problem.

`forcescon.m` (function):

Calculates the constraints of the optimization problem.

`tacpoint.m` (Script):

Creates the point cloud of the DLR robotic fingertips and calculates the distances of all points from the four corner points.

`positionsxyz.m` (function):

Calculates the position of the contact point based on the sensor measurements transforming the coordinates of the tactile array into real coordinates.

`df_max.m` (function):

Calculates the influence of uncertainties on forces.

`dt_max.m` (function):

Calculates the influence of uncertainties on torqes.

`GrapsMatrix.m` (function):

Calculates the Grasp Matrix.

`linfr.m` (function):

Calculates the the linearized friction cone.

`linfr.m` (function):

Calculates the the linearized friction cone.

Bibliography

[1] C. S. Lovchik and M. A. Diftler. The robonaut hand: a dexterous robot hand for space. *Robotics and Automation, 1999. Proceedings. 1999 IEEE International Conference on*, 1999.

[2] J. Butterfass, M. Grebenstein, H. Liu, and G. Hirzinger. Dlr-hand ii: next generation of a dextrous robot hand. *Robotics and Automation, 2001. Proceedings 2001 ICRA. IEEE International Conference on*, 2001.

[3] H. Liu, P. Meusel, G. Hirzinger, M. Jin, Y. Liu, and Z. Xie. The modular multisensory dlr-hit-hand: Hardware and software architecture. *architecture,"Mechatronics, IEEE/ASME Transactions on*, 2008.

[4] H. Liu, K. Wu, P. Meusel, N. Seitz, G. Hirzinger, Y. W. Liu M. H. Jin, T. Lan S. W. Fan, and Z. P. Chen. Multisensory five finger dexterous hand: The dlr/hit hand ii. *International Conference on Intelligent Robots and Systems, IROS*, 2008.

[5] A. Sahbani, S. El-Khoury, and P. Bidaud. An overview of 3d object grasp synthesis algorithms. *Robotics and Autonomous Systems*, 2012.

[6] A. Bicchi. Hands for dexterous manipulation and robust grasping: a difficult road toward simplicity. *Robotics and Automation, IEEE Transactions on*, 2000.

[7] A. Bicchi. On the closure properties of robotic grasping. *International Journal of Robotics Research*, 1997.

[8] C. Ferrari and J. Canny. Planning optimal grasps. *Proceedings - IEEE International Conference on Robotics and Automation*, 1993.

[9] A. T. Miller and P. K. Allen. Examples of 3d grasp quality computations. *Proceedings - IEEE International Conference on Robotics and Automation*, 1999.

[10] B. Mishra. Grasp metrics: Optimality and complexity. 1995.

[11] R. Suarez, M. Roa, and J. Cornella. Grasp quality metrics. 2006.

[12] Y. Li, J. Fu, and N. Pollard. Data driven grasp synthesis using shape matching and task-based pruning. *IEEE Transactions on Visualization and Computer Graphics*, 2007.

[13] Y. Park and G. Starr. Optimal grasping using a multi
ngered robot hand. *IEEE International Conference on Robotics and Automation*, 1990.

[14] C. Xiong, Y. Li, Y.-L. Xiong, H. Ding, and Q. Huang. Grasp capability analysis of multifingered robot hands. *Robotics and Autonomous Systems*, 1999.

[15] C. Borst, M. Fischer, and G. Hirzinger. A fast and robust grasp planner for arbitrary 3d objects. *Proceedings - IEEE International Conference on Robotics and Automation*, 1999.

[16] L. Mangialardi, G. Mantriota, and A. Trentadue. A three dimensional criterion for the determination of optimal grip points. *Robotics and Computer-Integrated Manufacturing*, 1996.

[17] C. Xiong and Y. Xiong. Stability index and contact configuration planning for multifingered grasp. *Robotics and Computer Integrated Manufacturing*, 1998.

[18] M. Hershkovitz and M. Teboulle. Sensitivity analysis for a class of robotic grasping quality functionals. *Robotica*, 1998.

[19] G. Liu, J. Xu, X. Wang, and Z. Li. On quality functions for grasp synthesis, fixture planning and coordinated manipulation. *IEEE Transactions on Automation Science and Engineering*, 2004.

[20] R. D. Hester, M. Cetin, C. Kapoor, and D. Tesar. Criteria based approach to grasp synthesis. *Proceedings - IEEE International Conference on Robotics and Automation*, 1999.

[21] Z. Xue, J. Zoellner, and R. Dillmann. Automatic optimal grasp planning based on found contact points. *IEEE/ASME International Conference on*, 2008.

[22] Bruno Siciliano and Oussama Khatib, editors. *Springer Handbook of Robotics*. Springer, 2008. ISBN 978-3-540-23957-4.

[23] XiangYang Zhu and Jun Wang. Synthesis of force-closure grasps on 3-d objects based on the q distance. *Robotics and Automation, IEEE Transactions on*, 19(4): 669–679, 2003. ISSN 1042-296X. doi: 10.1109/TRA.2003.814499.

[24] Yun-Hui Liu, Miu ling Lam, and Dan Ding. A complete and efficient algorithm for searching 3-d form-closure grasps in the discrete domain. *Robotics, IEEE Transactions on*, 20(5):805–816, Oct 2004. ISSN 1552-3098. doi: 10.1109/TRO.2004.829500.

[25] M.A. Roa and R. Suarez. Computation of independent contact regions for grasping 3-d objects. *Robotics, IEEE Transactions on*, 25(4):839–850, 2009. ISSN 1552-3098. doi: 10.1109/TRO.2009.2020351.

[26] Yu Zheng and Wen-Han Qian. Coping with the grasping uncertainties in force-closure analysis. *I. J. Robotic Res.*, 24(4):311–327, 2005.

[27] R. Krug, D. Dimitrov, K. Charusta, and B. Iliev. On the efficient computation of independent contact regions for force closure grasps. In *Intelligent Robots and Systems (IROS), 2010 IEEE/RSJ International Conference on*, pages 586–591, 2010. doi: 10.1109/IROS.2010.5654380.

[28] M.A. Roa and R. Suarez. Influence of contact types and uncertainties in the computation of independent contact regions. In *Robotics and Automation (ICRA), 2011 IEEE International Conference on*, pages 3317–3323, 2011. doi: 10.1109/ICRA.2011.5980334.

[29] George I. Boutselis, C. P. Bechlioulis, M. V. Liarokapis, and K. J. Kyriakopoulos. An integrated approach towards robust grasping with tactile sensing. *Robotics and Automation, Proceedings. IEEE International Conference on*, 2014.

[30] Stephen L. Chiu. Task compatibility of manipulator postures. *I. J. Robotic Res.*, 7 (5):13–21, 1988.

[31] R. D. Hester, M. Cetin, C. Kapoor, and D. Tesar. A criteria-based approach to grasp synthesis. In *Robotics and Automation, 1999. Proceedings. 1999 IEEE International Conference on*, volume 2, pages 1255–1260 vol.2, 1999. doi: 10.1109/ROBOT.1999.772533.

[32] Jeffrey Kerr and Bernard Roth. Analysis of multifingered hands. *Research, The International Journal of Robotics*, 1986.

[33] M. Buss, H. Hashimoto, and J.B. Moore. Dextrous hand grasping force optimization. *Robotics and Automation, IEEE Transactions on*, 12(3):406–418, 1996. ISSN 1042-296X. doi: 10.1109/70.499823.

[34] Christoforos I. Mavrogiannis, Charalampos P. Bechlioulis, and Kostas J. Kyriakopoulos. Sequential improvement of grasp based on sensitivity analysis. *Proceedings - IEEE International Conference on Robotics and Automation*, 2013.

[35] P. Fungtammasan and T. Watanabe. Grasp input optimization taking contact position and object information uncertainties into consideration. *Robotics, IEEE Transactions on*, 28(5):1170–1177, 2012. ISSN 1552-3098. doi: 10.1109/TRO.2012.2197310.

[36] H. Liu, K. Wu, P. Meusel, N. Seitz, G. Hirzinger, M.H. Jin, Y.W. Liu, S.W. Fan, T. Lan, and Z.P. Chen. Multisensory five-finger dexterous hand: The dlr/hit hand ii. In *Intelligent Robots and Systems, 2008. IROS 2008. IEEE/RSJ International Conference on*, pages 3692–3697, 2008. doi: 10.1109/IROS.2008.4650624.

[37] M.V. Liarokapis, P.K. Artemiadis, and K.J. Kyriakopoulos. Functional anthropomorphism for human to robot motion mapping. In *RO-MAN, 2012 IEEE*, pages 31–36, 2012. doi: 10.1109/ROMAN.2012.6343727.

[38] Zhaopeng Chen, N.Y. Lii, T. Wimboeck, Shaowei Fan, Minghe Jin, C.H. Borst, and Hong Liu. Experimental study on impedance control for the five-finger dexterous robot hand dlr-hit ii. In *Intelligent Robots and Systems (IROS), 2010 IEEE/RSJ International Conference on*, pages 5867–5874, 2010. doi: 10.1109/IROS.2010.5649356.

[39] J. Friedman and T. Flash. Task-dependent selection of grasp kinematics and stiffness in human object manipulation. *Cortex*, 2007.

[40] T. Watanabe and T. Yoshikawa. Grasping optimization using a required external force set. *IEEE Transactions on Automation Science and Engineering*, 2007.

[41] M. Teichmann and B. Mishra. Probabilistic algorithms for efficient grasping and fixturing. *Algorithmica*, 2000.

[42] Z. Li and S. Sastry. Task-oriented optimal grasping by multifingered robotic hands. *IEEE J. Robotics and Automation*, 1988.

[43] Christoforos I. Mavrogiannis, Charalampos P. Bechlioulis, Minas V. Liarokapis, and Kostas J. Kyriakopoulos. Task-specific grasp selection for underactuated hands. *Robotics and Automation, Proceedings. IEEE International Conference on*, 2014.

[44] Richard M. Murray, S. Shankar Sastry, and Li Zexiang. *A Mathematical Introduction to Robotic Manipulation*. CRC Press, Inc., Boca Raton, FL, USA, 1st edition, 1994. ISBN 0849379814.

[45] David G. Kirkpatrick, Bhubaneswar Mishra, and Chee-Keng Yap. Quantitative steinitz's theorems with applications to multifingered grasping. pages 341–351. ACM, 1990.